Available online at www.sciencedirect.com
ScienceDirect

ELSEVIER

Coordination Chemistry Reviews 251 (2007) 1493–1520

COORDINATION
CHEMISTRY REVIEWS

www.elsevier.com/locate/ccr

Review

Structures and luminescent properties of lanthanide phosphonates

Jiang-Gao Mao

State Key Laboratory of Structural Chemistry, Fujian Institute of Research on the Structure of Matter, Chinese Academy of Sciences, Fuzhou 350002, PR China

Received 11 October 2006; accepted 10 February 2007

Contents

Abstract

The crystal structures and luminescent properties of lanthanide phosphonates are reviewed. The structural elucidation for lanthanide phosphonates is difficult due to its low solubility and poor crystallinity. To overcome these problems, two types of synthetic techniques were applied: attaching various functional groups or introducing a second metal linker. By attaching various types of functional groups to the phosphonate ligand, lanthanide phosphonates with 0D, 1D, 2D and 3D structures have been isolated. Using the acidic metal linker such as oxalate usually leads to compounds with a complicated 3D network structure whereas a basic second metal linker such as phen helps the formation of compounds containing the polynuclear clusters. Phosphonic acids are versatile ligands that can adopt a number of coordination modes depending on the cation size, temperature and the pH value of the reaction media. The luminescence properties of some lanthanide phosphonates are also discussed.

Keywords: Syntheses; Crystal structures; Rare earth phosphonates; Open frameworks; Luminescence

1. Introduction

During the last two decades great effort has been devoted to the design and synthesis of metal phosphonates with novel open framework or microporous structures due to their potential applications in electro-optical, ion-exchange, catalysis and sensors [1]. The strategy of attaching functional groups such as crown ether, amine, hydroxyl, or/and carboxylate groups to the phosphonic acid has proven to be very effective for the isolation of a variety of metal phosphonates with open framework and microporous structures [2–21]. Most of the studies have been focused on first row transition metals, zirconium(IV) as well as main group metals such as Al(III), Ga(III) and Pb(II) [1–21], and a number of good reviews are available [1,22–24]. Reports on lanthanide phosphonates are rather limited and some of them were based on X-ray powder diffraction. So far the chemistry of lanthanide phosphonates has not yet been reviewed.

Lanthanide phosphonates normally have low solubility in water and organic solvents, hence it is difficult to obtain single crystals suitable for X-ray structural analysis. Nevertheless the elucidation of the structures of lanthanide phosphonates is very important since these compounds may exhibit useful luminescent properties in both the visible and near IR regions [25,26]. To improve the solubility and crystallinity of lanthanide phosphonates, additional functional groups such as crown ether, carboxylate, hydroxyl and amine groups have been attached to the phosphonic acid. In particular we, as well as others, found

---

E-mail address: mjg@ms.fjirsm.ac.cn.

0010-8545/$ – see front matter © 2007 Elsevier B.V. All rights reserved.
doi:10.1016/j.ccr.2007.02.008

that phosphonic acid containing an amino-carboxylic acid moiety is very useful for the design of lanthanide phosphonates with novel architectures and luminescent properties [45,49,53]. Such a ligand is very versatile and can adopt a variety of coordination modes depending on the cation size, pH value of the reaction media as well as reaction temperature. Another successful approach proposed and adopted by our group is to introduce a second metal linker such as oxalate anion or phen. We can solve the solubility and crystallinity problems by introducing an acidic second ligand, in the meantime we can also enhance luminescent intensity and lifetime of the resultant lanthanide complexes through the so-called "antenna effect". By using $MeN(CH_2CO_2H)(CH_2PO_3H_2)$ as the main ligand and 5-sulfoisophthalic acid as the second ligand we prepared a series of layered lanthanide-sulfonate-carboxylate-phosphonate hybrids [61]. Using oxalate instead of 5-sulfoisophthalic acid led to a series of lanthanide phosphonates with novel 3D network structures [62]. Later we extended this approach to the lanthanide tetraphosphonate system in which the solubility and crystallinity problems are much worse, again it turned out to be a success [63]. Very recently we also used a basic ligand such as phen as the second ligand. By using a phosphonate ligand functionalized by the sulfonate group (*m*-sulfophenylphosphonic acid), we successfully isolated a series of lanthanide compounds featuring various types of tetranuclear lanthanide phosphonate-sulfonate cluster units [64]. This review summarizes the structural chemistry and luminescent properties of lanthanide phosphonates, including those containing additional functional groups or second metal linkers. The structures and abbreviations for some of the phosphonic acids used are presented in Scheme 1. In the following sections, the discussion of lanthanide phosphonates will be in the order by the functional groups attached.

2. Lanthanide complexes with aryl- or alkyl-substituted phosphonic acids

Lanthanide phosphonates in this category are listed in Table 1. The first lanthanide phosphonates reported were prepared in 1990 by Mallouk and coworkers [27]. They prepared the cerium and lanthanum phenylphosphonates with composition $Ln(O_3PC_6H_5)(HO_3PC_6H_5)$ and a series of alkylphosphonates such as $Ln(O_3PMe)(HO_3PMe)$. From the unit cell parameters they deduced that the structures of these lanthanide phosphonates were most likely related to those of $Ca(HO_3PR)_2$ and $Zr(O_3PR)_2$ ($R = Me$, C_6H_5–) both having a layered structure [27]. Two years later, the structures of $La(O_3PC_6H_5)(HO_3PC_6H_5)$ and $La(O_3PCH_2C_6H_5)(HO_3PCH_2C_6H_5)(H_2O)_2$ were elucidated by Clearfield and coworkers [28]. The La(III) ion in $La(O_3PC_6H_5)(HO_3PC_6H_5)$ is 8-coordinate with eight phosphonate oxygen atoms. Each phosphonate group forms a La–O–P–O chelating ring with a La(III) ion, one oxygen of the chelating ring and the third phosphonate oxygen each bridges with an adjacent metal ion. Such connectivity resulted in a layered structure with the phenyl ring oriented toward the interlayer space (Fig. 1). In $La(O_3PCH_2C_6H_5)(HO_3PCH_2C_6H_5)(H_2O)_2$, only six oxygen atoms of the metal coordination sphere are provided by the phosphonate ligands, the remaining two are from aqua ligands. The deprotonated phosphonate group adopts the same coordination mode as in $La(O_3PC_6H_5)(HO_3PC_6H_5)$. The protonated phosphonate group bridges with two La(III) ions using two oxygen atoms. The third oxygen atom with a longer P–O distance remains uncoordinated. The interlayer distance of 16.6 Å is slightly larger than that for $La(O_3PC_6H_5)(HO_3PC_6H_5)$ (15.7 Å) due to the additional CH_2 group (Fig. 1b).

Two scandium methylphosphonates were prepared hydrothermally and their structures determined [29]. The crystallinity of the solids was improved by adding hydrogen fluoride or sodium hydroxide as a mineralizing agent. $ScF(H_2O)CH_3PO_3$ is a non-porous solid built up from corner-sharing ScF_2O_4 octahedral chains interlinked by methylphosphonate ligands. The ScO_4F_2 octahedra are interconnected by sharing fluoride anions into a 1D chain along the *a*-axis (Fig. 2a). There is no free volume in the structure. The structure of $NaSc(CH_3PO_3)_2{\cdot}0.5H_2O$ was solved *ab initio* from high-resolution synchrotron X-ray powder diffraction data. It has a fully connected, negatively charged scandium phosphonate framework where ScO_6 octahedra share vertices with phosphonate groups. The sub-units of the framework can be considered as double columns of ScO_6 octahedra parallel to the *c*-axis, linked by phosphonate groups. These are connected in rings of four by additional phosphonate groups around the smaller inorganic channels (Fig. 2b). There are two channel systems in the inorganic framework running parallel to the *c*-axis, one surrounded by 4 Sc and 4 P, the other by 8 Sc and 8 P. The channel ringed by 8 Sc and 8 P is lined by methyl groups, leaving little void space. The channels surrounded by 4 Sc and 4 P are fully inorganic in nature, and are large enough to accommodate water bound to extra framework sodium cations. The sodium cations are located at the smaller channels and their coordination spheres are completed by aqua ligands, which may be reversibly removed and adsorbed.

Table 1
Lanthanide complexes with aryl- and alkyl-substituted phosphonic acids

Compound	Structural features	References
$Ln(O_3PC_6H_5)(HO_3PC_6H_5)$ ($Ln = La, Ce$)	Layered	[27,28]
$La(O_3PMe)(HO_3PMe)$	Layered	[27]
$La(O_3PCH_2C_6H_5)(HO_3PCH_2C_6H_5)(H_2O)_2$	Layered	[28]
$ScF(H_2O)(CH_3PO_3)$	3D network	[29]
$NaSc(CH_3PO_3)_2{\cdot}0.5H_2O$	3D network	[29]
$LnH[O_3P(CH_2)_nPO_3]$ ($n = 1$–3; Ln = Pr, Nd, Eu, Gd)	Pillared layered	[30–32]
$[Ln(H_2L^1)(H_3L^1)(H_2O)_4]{\cdot}xH_2O$ (Ln = La, Ce, Pr, Nd, Sm, Gd, Tb; $x = 9$–14)	Layered	[33]

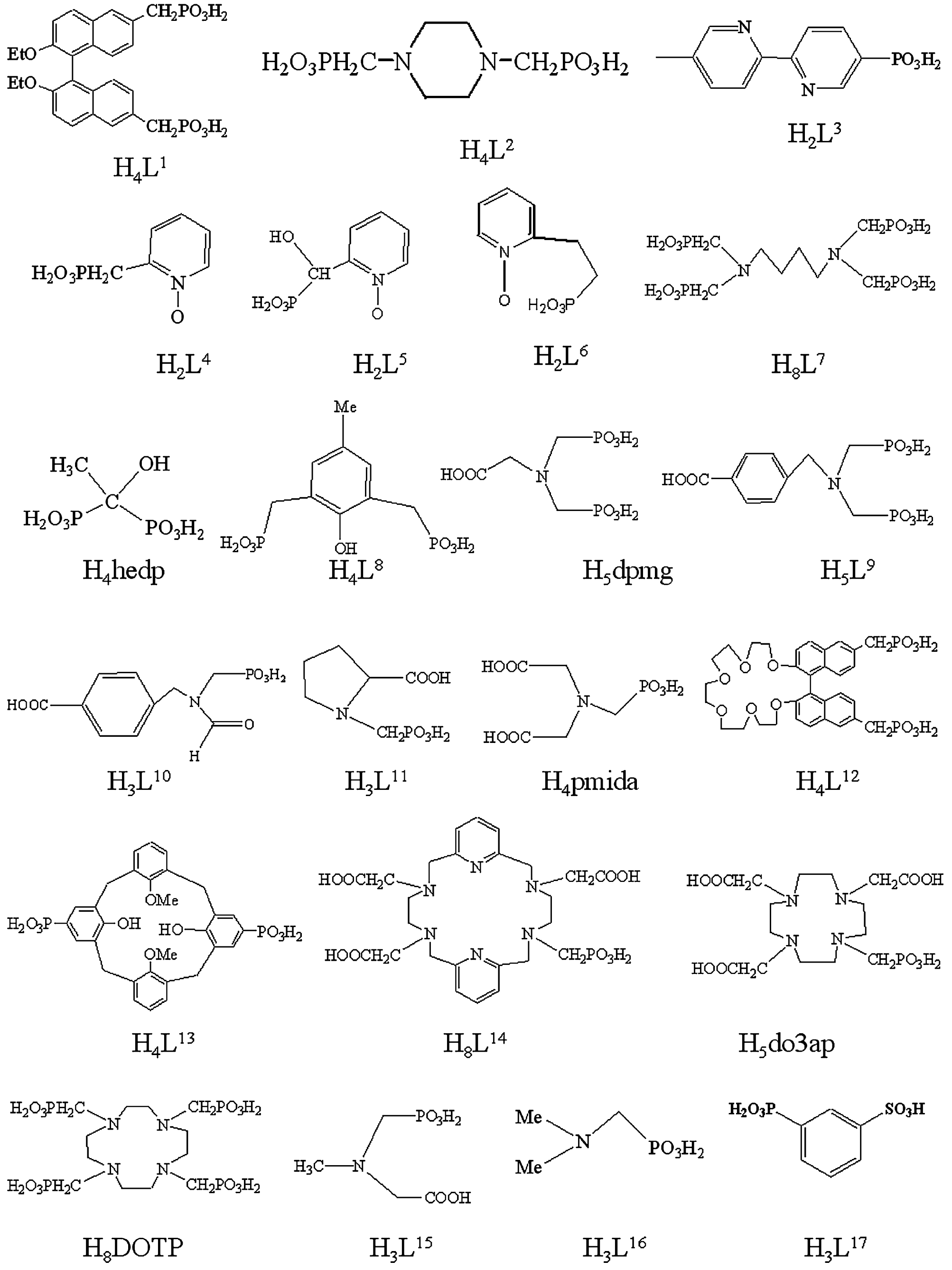

Scheme 1. Phosphonic acids in some lanthanide compounds.

A series of lanthanide organodiphosphonates with 3D networks, $LnH[O_3P(CH_2)_nPO_3]$ (n = 1–3; Ln = Pr, Nd, Eu, Gd) was structurally determined from X-ray powder diffraction studies [30–32]. Despite the different lengths of the carbon chain, all these compounds display a similar pillared layered architecture. The lanthanide(III) ion is 8-coordinate and each phosphonate group is tetradentate, chelating in a bidentate fashion with a lanthanide ion and bridging with two additional lanthanide(III) ions (Fig. 3a). Each pair of Ln(III) ions is bridged by a pair of oxygen atoms into a 1D chain, and neighboring chains are bridged by phosphonate groups into an inorganic layer. Neighboring inorganic layers are further interconnected by the carbon chains of the phosphonate ligands (Fig. 3b). The length of the carbon chain has a dramatic effect on the interlayer distances, which are about 9.6, 8.0 and 7.0 Å, respectively for n = 3, 2, 1. Under 457.9 nm argon ion laser excitation at 77 K, $EuH[O_3P(CH_2)_3PO_3]$ displayed a weak band at 580 nm for the $^5D_0 \rightarrow {}^7F_0$ transition, three moderate lines for the $^5D_0 \rightarrow {}^7F_1$ transition in the wavelength range 590–595 nm, five strong lines for the $^5D_0 \rightarrow {}^7F_2$ transition in the wavelength range 610–622 nm and seven weak lines for the $^5D_0 \rightarrow {}^7F_4$ transition [32]. These results confirm the low symmetry of the europium(III) site.

By slow evaporation of an acidic mixture of lanthanide nitrate or perchlorate salt and 2,2′-diethoxy-1,1′-

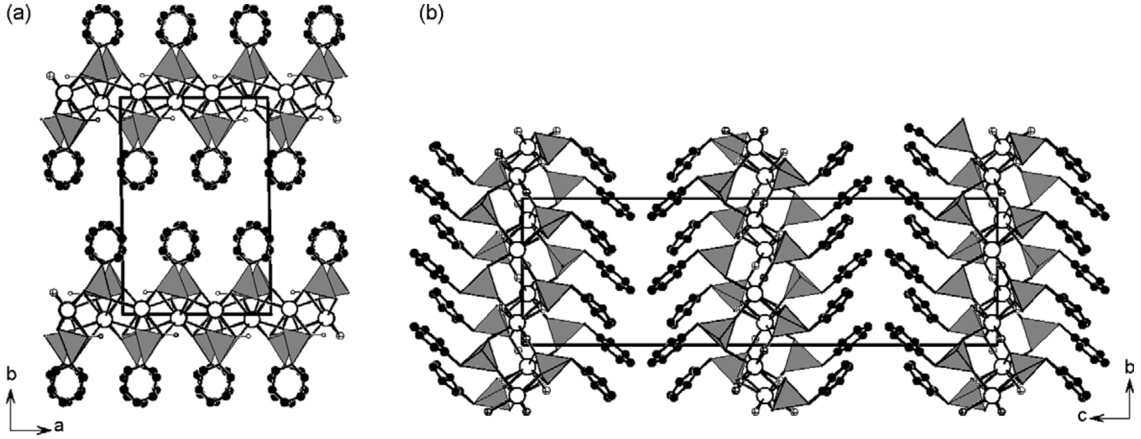

Fig. 1. Structures of $La(O_3PC_6H_5)(HO_3PC_6H_5)$ (a) and $La(O_3PCH_2C_6H_5)(HO_3PCH_2C_6H_5)(H_2O)_2$ (b). In all figures unless specified the phosphonate groups are shaded in gray, Ln, C and O are drawn as open, black and crossed circles, respectively (adapted from Ref. [28]).

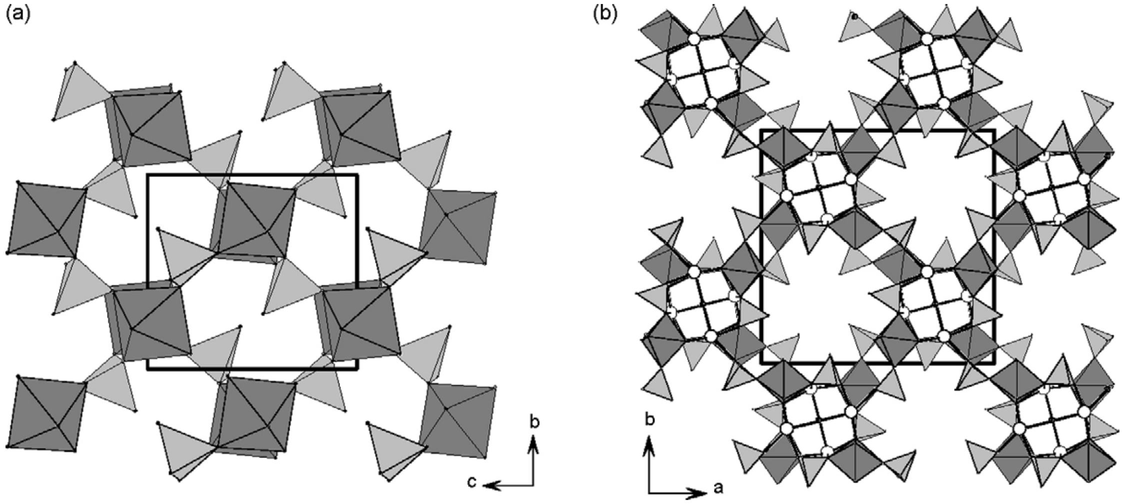

Fig. 2. Structure of $ScF(H_2O)(CH_3PO_3)$ viewed down *a*-axis (a) and the open framework of $NaSc(CH_3PO_3)_2\cdot0.5H_2O$ (b). Sc coordination octahedra and PO_3C tetrahedra are shaded in dark and light gray, respectively (adapted from Ref. [29]).

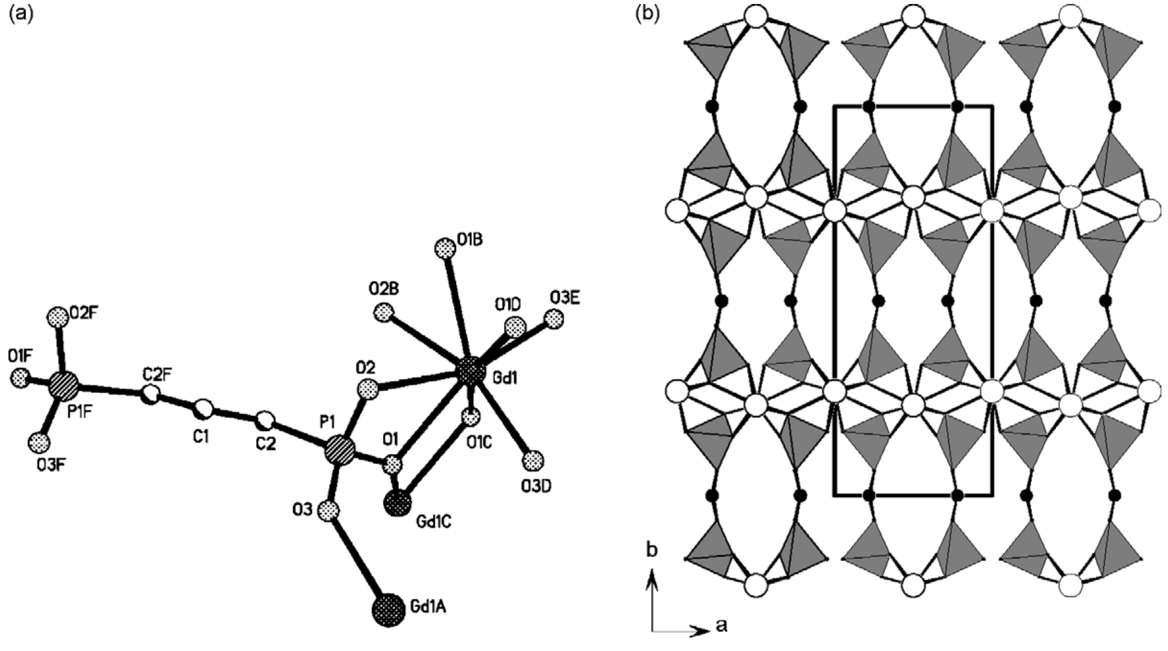

Fig. 3. The selected unit (a) and structure of $GdH(O_3PCH_2CH_2CH_2PO_3)$ (b) (adapted from Ref. [32]).

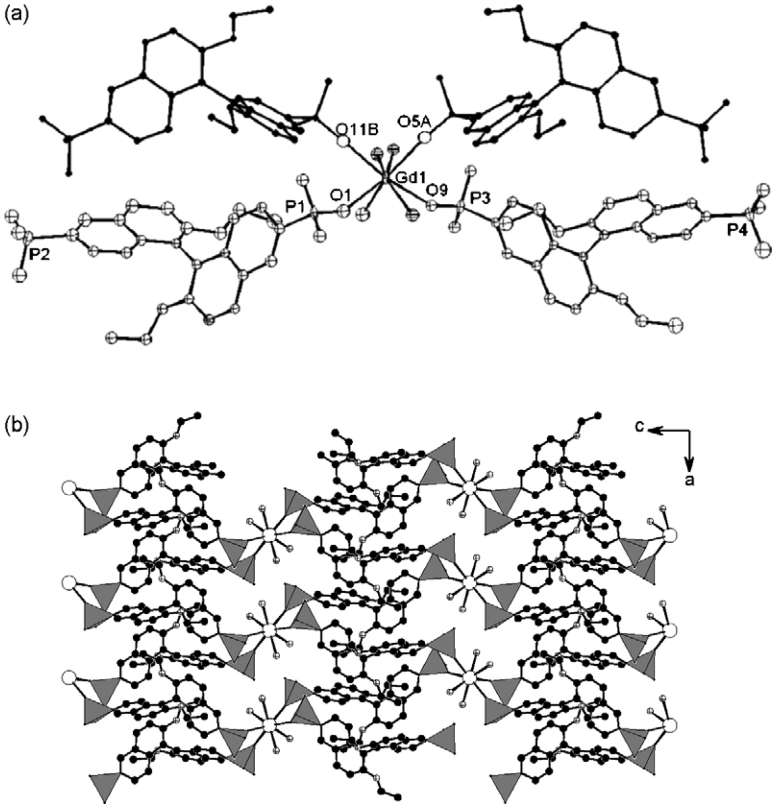

Fig. 4. The selected unit (a) and a view of 2D framework of $[Gd(H_2L^1)(H_3L^1)(H_2O)_4]\cdot 12H_2O$ (b) (adapted from Ref. [33]).

binaphthalene-6,6′-bisphosphonic acid (H_4L^1), a series of homochiral lanthanide bisphosphonates with the general formula $[Ln(H_2L^1)(H_3L^1)(H_2O)_4]\cdot xH_2O$ (Ln = La, Ce, Pr, Nd, Sm, Gd, Tb, x = 9–14) were synthesized by the Lin group [33]. The lanthanide(III) center is 8-coordinate with four phosphonate oxygen atoms from four bisphosphonates ligands and four aqua ligands (Fig. 4a). All four phosphonate groups are monodentate, three of them are 1H-protonated whereas the fourth one is doubly protonated. The interconnection of Ln(III) ions by bridging bisphosphonate ligands led to a 2D layer with the binaphthyl rings oriented toward the interlayer space (Fig. 4b). The packing of such layers leaves large asymmetric channels with a largest dimension of ~12 Å. These compounds could be possibly used in heterogeneous catalysis and chiral separation based on experiments [33].

In summary, the lanthanide complexes with aryl or alkyl substituted mono-phosphonic acids normally display a layered structure whereas those of the corresponding di-phosphonic acids prefer a pillared-layered structure. The inclusion of fluorine anion or sodium cation in the framework can lead to new types of open framework structures.

3. Lanthanide complexes with phosphonic acids functionalized with hydroxyl or amine groups

The structurally characterized lanthanide phosphonates in this group are listed in Table 2. The first lanthanide aminophosphonate, $Lu(HO_3PCH_2CH_2NH_3)_3\ (ClO_4)_3\cdot 3D_2O$ was reported by Legendziwicz in 1999 [34]. Its structure features a 1D lutetium(III) phosphonate chain (Fig. 5). The Lu(III) ion is octahedrally coordinated with six phosphonate oxygen atoms from six phosphonate ligands. The Lu–O distances are quite similar, ranging from 2.194(6) to 2.210(5) Å. The counteranions and the solvent molecules are not involved in metal coordination. The phosphonate group is bidentate bridging, the third phosphonate oxygen atom and the amine group are protonated and remain uncoordinated. Each pair of Lu(III) ion is bridged by three phosphonate groups into a 1D inorganic chain.

Two novel 3D lanthanum phosphonates, $[La_2(H_2L^2)(H_4L^2)]Cl_2$ and $[La_2(H_2L^2)_2(H_3L^2)]Cl$, were prepared by using an amino-diphosphonic acid derived from piperazine,

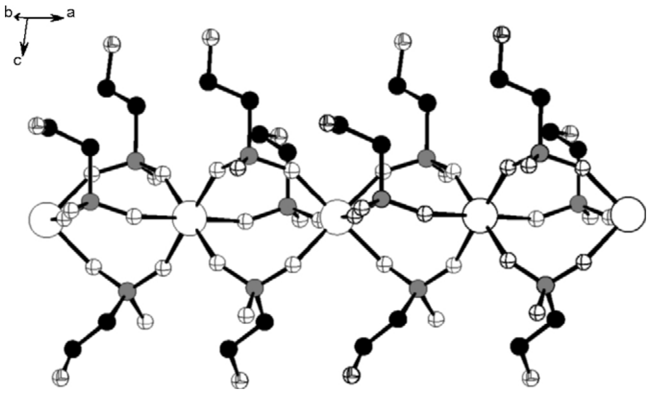

Fig. 5. The 1D chain in $Lu(HO_3PCH_2CH_2NH_3)_3(ClO_4)_3\cdot 3D_2O$. P and N atoms are drawn as gray and hatched circles (adapted from Ref. [34]).

Table 2
Lanthanide complexes of phosphonic acids attached by amine or hydroxyl groups

Compound	Structural features	Reference
$Lu(HO_3PCH_2CH_2NH_3)_3(ClO_4)_3\cdot 3D_2O$	1D chain	[34]
$[La_2(H_2L^2)(H_4L^2)]Cl_2$	3D network	[35]
$[La_2(H_2L^2)_2(H_3L^2)]Cl$	3D network	[35]
$Ln_2(H_2L^2)_3\cdot nH_2O$ (Ln = Gd, $n = 3$; Ln = Y, $n = 5$; Ln = Nd, $n = 9$)	1D chain	[36]
$[Na_6Eu_9(L^3)_{16}](OH)\cdot 51H_2O$	Cluster	[37]
$Gd\{(4\text{-}C_5H_4N)CH(OH)PO_3H\}_3\cdot 6H_2O$	1D chain	[38]
$Er(HL)_3(H_2L)\cdot 8H_2O$ ($L = L^4$ or L^5)	Molecular units	[39]
$Nd(HL^6)_3$	1D chain	[40]
$Gd(H_5L^7)\cdot 2H_2O$	Layered	[41]
$Ln(H_3hedp)(H_2hedp)_2\cdot 5H_2O$ (Ln = Y, Tb, Dy, Er, Tm, Yb, Lu)	1D chain	[42]
$[H_3O]Eu(H_2hedp)_2\cdot 12H_2O$	1D chain	[42]
$Nd(H_3hedp)(H_2hedp)_2\cdot 7H_2O$	1D chain	[42]
$Gd(Hhedp)(H_2O)_2\cdot H_2O$	Layered	[43]
$La(HL^8)(H_2O)_2$	Layered	[44]

$H_2O_3PCH_2N(C_2H_4)_2NCH_2PO_3H_2(H_4L^2)$ [35]. The structures of both compounds are based on similar 1D lanthanum(III) phosphonate inorganic chains interconnected via organic groups of the phosphonate ligands. The chloride anions in both compounds are located at tunnels along the *a*-axis (Fig. 6).

The La(III) ions in $[La_2(H_2L^2)(H_4L^2)]Cl_2$ are 8-coordinate with eight phosphonate oxygen atoms from seven phosphonate groups (Fig. 6a). There are two types of phosphonate ligands: one is a zwitterion (neutral) and the other is doubly protonated. The amine groups in both types of ligands are protonated. Both phosphonate groups in the neutral ligand are unidentate and singly protonated. The two phosphonate groups of the $(H_2L^2)^{2-}$ anion are fully deprotonated, one is tridentate and bridges to three La(III) ions whereas the other one is tetradentate, being chelating in a bidentate fashion with a La(III) ion and also bridging with two additional metal ions by using one chelating oxygen and the third phosphonate oxygen atom. Among two independent La(III) ion in $[La_2(H_2L^2)_2(H_3L^2)]Cl$, one is 7-coordinate and the other one is 8-coordinate (Fig. 6c). One $[H_2L]^{2-}$ anion adopts the same coordination mode as in $[La_2(H_2L^2)(H_4L^2)]Cl_2$, whereas the other one bridges with six La(III) ions. The $(H_3L^2)^-$ anion bridges with two La(III) ions by using two phosphonate groups. The La(III) ions in both compounds are bridged by phosphonate groups into 1D inorganic chains along *a*-axis, which are further interconnected by organic groups of the phosphonate ligands into 3D open frameworks (Fig. 6b and d). However, the connectivities between chains are different: each chain is bridged to six neighboring chains in $[La_2(H_2L^2)(H_4L^2)]Cl_2$ whereas each chain is bridged to only four neighboring chains in $[La_2(H_2L^2)_2(H_3L^2)]Cl$. The number of incorporated counter anions is mainly responsible for the two different polytypic structures [35]. Under similar reaction conditions, Lightfoot et al. also isolated three other lanthanide(III) compounds, $Gd_2(H_2L^2)_3\cdot 3H_2O$, $Y_2(H_2L^2)_3\cdot 5H_2O$ and $Nd_2(H_2L^2)_3\cdot 9H_2O$ [36]. 1D 'lanthanide-phosphate' chains are a key feature in all structures, although there are major structural differences between the chains. Both Gd(III) and Y(III) compounds display octahedral LnO_6 coordination whereas Nd(III) compound shows eight-coordination NdO_8 polyhedra. The inorganic chains in Gd(III) and Y(III) compounds are similar to those in $Lu(HO_3PCH_2CH_2NH_3)_3(ClO_4)_3\cdot 3D_2O$ [34]. In the inorganic chain of $Nd_2(H_2L^2)_3\cdot 9H_2O$, neighboring neodymium(III) ions are alternatively bridged by four and two phosphonate groups (Fig. 7). In each case, 3D connectivity is completed by the coordination of the phosphonate group, resulting in an open framework structure encapsulating loosely bound water molecules. It was also shown that the extra-framework water molecules in Y(III) compound may be removed reversibly without framework collapse [36].

Bünzli and coworkers reported an interesting europium(III) complex with 5′-methyl-2,2′-bipyridyl-6-phosphonic acid (H_2L^3), $[Na_6Eu_9(L^3)_{16}](OH)\cdot 51H_2O$ [37]. Its structure feature is a $\{Eu_9Na_6(L^3)_{16}\}^+$ cluster unit (Fig. 8). Eight Eu(III) ions form an irregular circle whereas the remaining one is disordered and located at the center of the circle. Three sodium(I) ions are bridged by two bridging phosphonate oxygen atoms into a trimer. Neighboring Na_6Eu_9 clusters are held together by an intricate network of bridging phosphonate groups. In addition, sizable π–π interactions occur between one pyridine of pairs of parallel ligand strands, with a mean distance of 3.42 Å. The quantum yield measured on polycrystalline samples upon ligand excitation at 30,300 cm^{-1} is as high as 32 ± 5%. The isomorphous complexes containing the $Na_6Eu_{9-x}Yb_x$ ($x = 4$ and 5) clusters display dual luminescence in the visible (Eu^{III}) and NIR (Yb^{III}) ranges (Fig. 9).

The Gadolinium complex of the [hydroxy(4-pyridyl)methyl] phosphonate ligand, $Gd\{(4\text{-}C_5H_4N)CH(OH)PO_3H\}_3\cdot 6H_2O$ reported by Zheng and coworkers [38] has a 1D chain structure in which each pair of GdO_6 octahedra is bridged by three O–P–O linkages. The amine and the hydroxyl groups of the ligand are not involved in metal coordination but participate in the interchain hydrogen bonding. Paine and coworkers synthesized two new phosphonic acids based on 2-pyridyl *N*-oxide, 2-(pyridyl *N*-oxide) methylphosphonic acid (H_2L^4) and 2-(pyridyl *N*-oxide) hydroxymethylphosphonic acid (H_2L^5) [39]. Reaction of these ligands with freshly prepared erbium hydroxide resulted in two isostructural complexes, namely, $Er(HL)_3(H_2L)\cdot 8H_2O$ ($L = L^4$ or L^5). The erbium(III) ion is 8-coordinate with four in a biden-

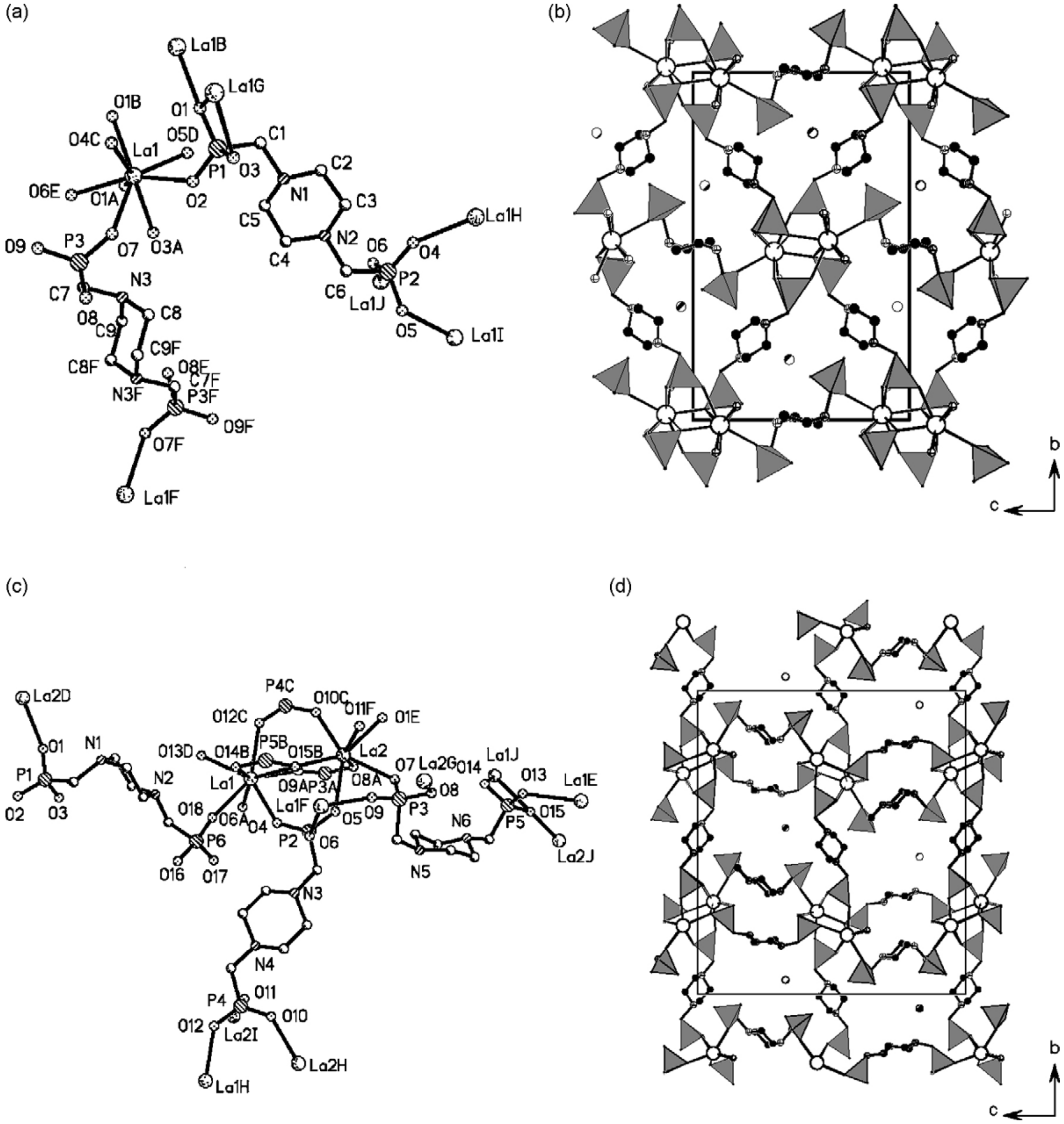

Fig. 6. The selected unit of $[La_2(H_2L^2)(H_4L^2)]Cl_2$ (a), view of the structures of $[La_2(H_2L^2)(H_4L^2)]Cl_2$ down the *a*-axis (b), the selected unit of $[La_2(H_2L^2)_2(H_3L^2)]Cl$ (c) and $[La_2(H_2L^2)_2(H_3L^2)]Cl$ down the *a*-axis (d). The small open circles represent Cl^- anions (adapted from Ref. [35]).

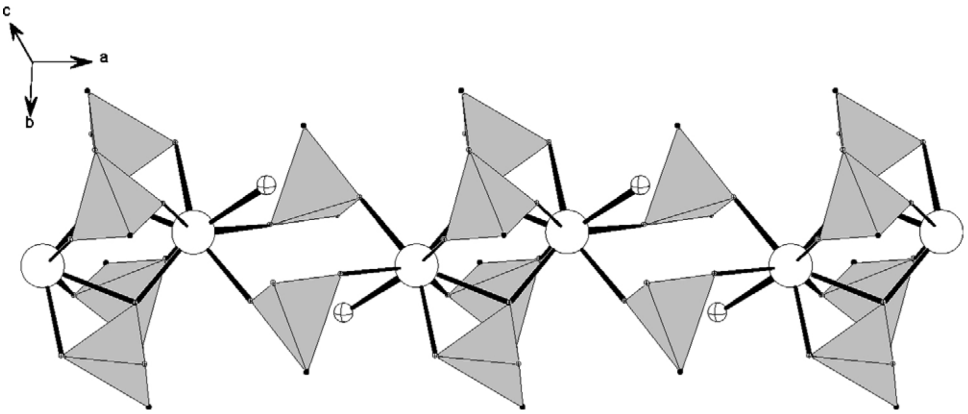

Fig. 7. The 1D inorganic chain in $Nd_2(H_2L^2)_3{\cdot}9H_2O$ (adapted from Ref. [36]).

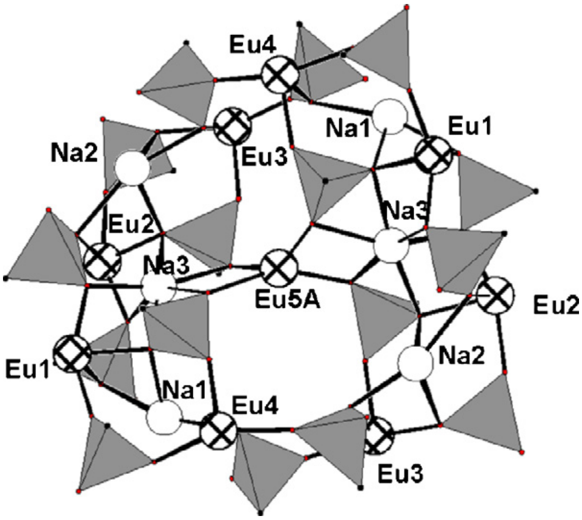

Fig. 8. The $\{Eu_9Na_6(L^3)_{16}\}^+$ cluster unit (adapted from Ref. [37]).

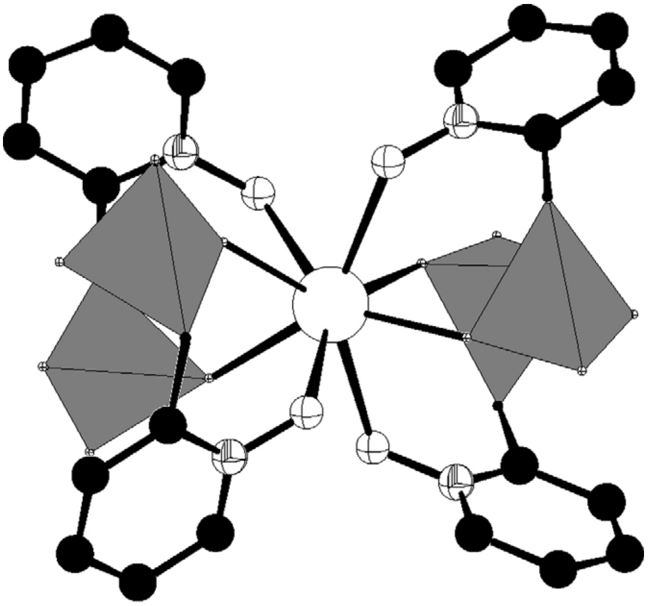

Fig. 10. Molecular structure of $Er(HL^5)_3(H_2L^5){\cdot}8H_2O$ (adapted from Ref. [39]).

tate fashion chelating phosphonate ligands (Fig. 10), three of which are 1H-protonated and the fourth one is neutral. Each phosphonate ligand forms a seven-member chelating ring with an erbium(III) ion by using one phosphonate oxygen and one oxygen atom from the *N*-oxide group. These molecular units of $Er(HL)_3(H_2L){\cdot}8H_2O$ ($L = L^4$ or L^5) are further interconnected by extensive hydrogen bonds into a 3D structure. When 2-(2-pyridyl-*N*-oxide) ethylphosphonic acid (H_2L^6) was used, the non-hydrated $Nd(HL^6)_3$ was isolated [40]. Each ligand is bidentate bridging by using two phosphonate oxygen atoms, the third one is protonated and is only involved in hydrogen bonding. No chelating ring is formed, which may be due to the fact that an 8-membered chelating ring is very unstable. The Nd(III) ion sits on sites with -3 symmetry and it is octahedrally coordinated with six phosphonate oxygen atoms from six ligands. Neighboring two Nd(III) ions are bridged by three phosphonate groups into a 1D chain along *c*-axis.

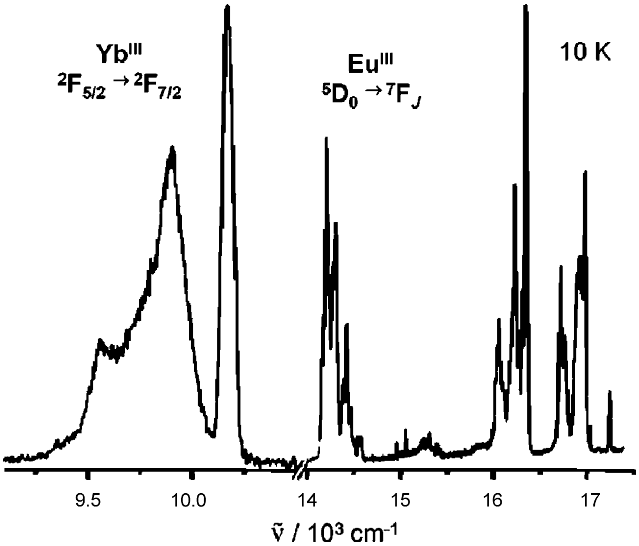

Fig. 9. Luminescence spectra at 10 K [ν_{ex}] 28,180 (left region) and 21,468 cm^{-1} (right region) of the polycrystalline $Na_6Eu_{9-x}Yb_x(L^3)_{16}$ cluster showing emission of both Yb^{III} and Eu^{III} (adapted from Ref. [37]).

The hydrothermal reaction of $(H_2O_3PCH_2)_2N{-}(CH_2)_4{-}N(CH_2PO_3H_2)_2$ (H_8L^7) with gadolinium(III) nitrate afforded a layered compound, $Gd(H_5L^7){\cdot}2H_2O$ [41]. The Gd(III) ion is 8-coordinate with eight phosphonate oxygen atoms from five different phosphonate groups of five different phosphonic ligands (Fig. 11a). Each Gd atom is connected with its neighboring Gd atoms through two phosphonate oxygen atoms, forming a gadolinium phosphonate slab along the *a*-axis. Such slabs are bridged by tetraphosphonate $(H_5L^7)^{3-}$ anions into a 2D layer (Fig. 11b). These layers are further interlinked by strong hydrogen bonds formed between uncoordinated phosphonate oxygen atoms into a 3D supermolecular structure. Luminescent studies indicate that this compound exhibits a broad blue fluorescent emission band at 441 nm [41].

Using 1-hydroxyethane-1,1-diphosphonic acid (H_4hedp) as a phosphonate ligand, a series of lanthanide complexes was isolated by Nash et al., namely, $Ln(H_3hedp)(H_2hedp)_2{\cdot}5H_2O$ (Ln = Y, Tb, Dy, Er, Tm, Yb, Lu), $[H_3O]Eu(H_2hedp)_2{\cdot}12H_2O$ and $Nd(H_3hedp)(H_2hedp)_2{\cdot}7H_2O$ [42]. The light lanthanide compounds contain more lattice water molecules. All these compounds feature a 1D inorganic chain. Eu(III) and Nd(III) ions are 8-coordinate whereas the heavier lanthanide ions are 7-coordinate. Neighboring two 8-coordinate lanthanide(III) ions are bridged by four phosphonate groups whereas a pair of 7-coordinate lanthanide(III) ions are bridged alternatively by two and four phosphonate groups [42]. The hydroxyl group is only involved in the intra-chain hydrogen bonding (Fig. 12).

When the Ln/L ratio is 1:1, Lee and coworkers reported a layered gadolinium(III) complex, $Gd(Hhedp)(H_2O)_2{\cdot}H_2O$ [43]. The gadolinium(III) ion is 8-coordinate with six phosphonate oxygen atoms and two aqua ligands. One phosphonate group of

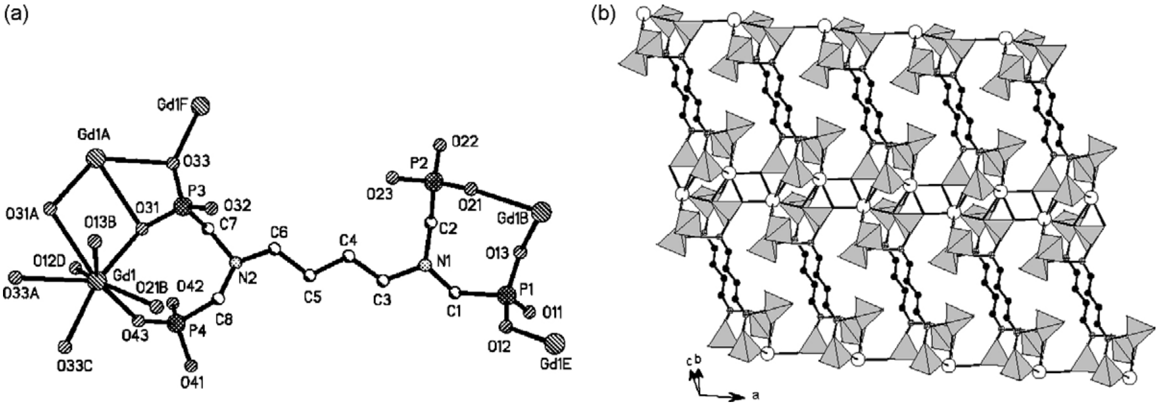

Fig. 11. The selected unit (a) and a 2D layer in Gd(H_5L^7)·$2H_2O$ (b) (adapted from Ref. [41]).

the ligand is fully deprotonated and bridges with four Gd(III) ions whereas the other one is 1H-protonated and connects with two Gd(III) ions. Along the *a*-axis, each pair of Gd(III) ions are interconnected alternatively by a pair of phosphonate groups (Gd–$(O–P–O)_2$–Gd bridge) and a pair of phosphonate oxygen atoms (Gd–O–Gd bridge) into a 1D chain, such chains are further cross-linked by phosphonate ligands into a 2D layer (Fig. 13). The hydroxyl group of the ligand remains uncoordinated and is involved in the interlayer hydrogen bonding with lattice water.

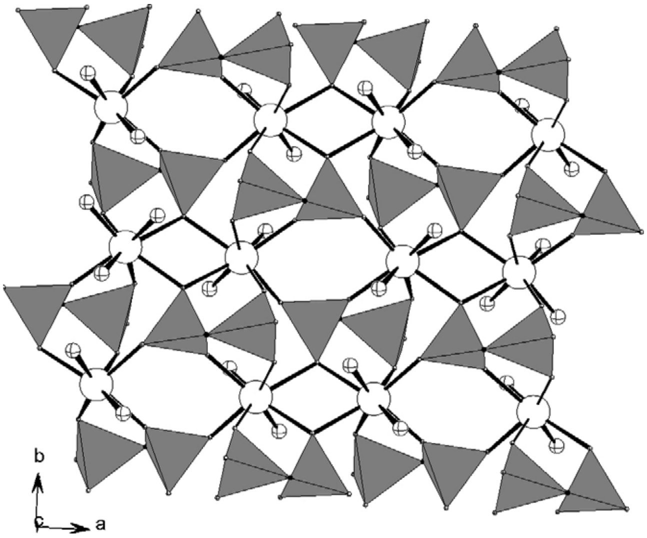

Fig. 13. A 2D Gd(III) phosphonate layer in Gd(Hhedp)$(H_2O)_2$·H_2O. The hydroxyl groups were omitted for clarity (adapted from Ref. [43]).

La(HL^8)$(H_2O)_2$ was prepared by reacting H_4L^8 and lanthanide chloride in dilute (0.02 M) HCl at 125 °C [44] and has a layered structure (Fig. 14). The lanthanum(III) ion is 8-coordinate with six phosphonate oxygen atoms from four phosphonate anions and two aqua ligands with La–O distances ranging from 2.393(2) to 2.646(2) Å. Each phosphonate ligand acts as a hexadentate metal linker. It chelates with a La(III) ion in a bidentate fashion by using two oxygen atoms from two phosphonate groups, chelates with another La(III) ion in a bidentate fashion by using two oxygen atoms from a same phosphonate group and also bridges with two other La(III) ions by using two of the three remaining phosphonate oxygen atoms (Fig. 14a). The uncoordinated phosphonate oxygen is protonated. The hydroxyl group attached to the benzene ring is also uncoordinated. The La(III) ions are interconnected by bidentate and tridentate bridging phosphonate groups into a layered architecture (Fig. 14b). The organic groups of the phosphonate groups hang on both sides of the inorganic layer. There is only weak van der Waals force between neighboring layers (Fig. 14b). The interlayer space is about 12 Å [44].

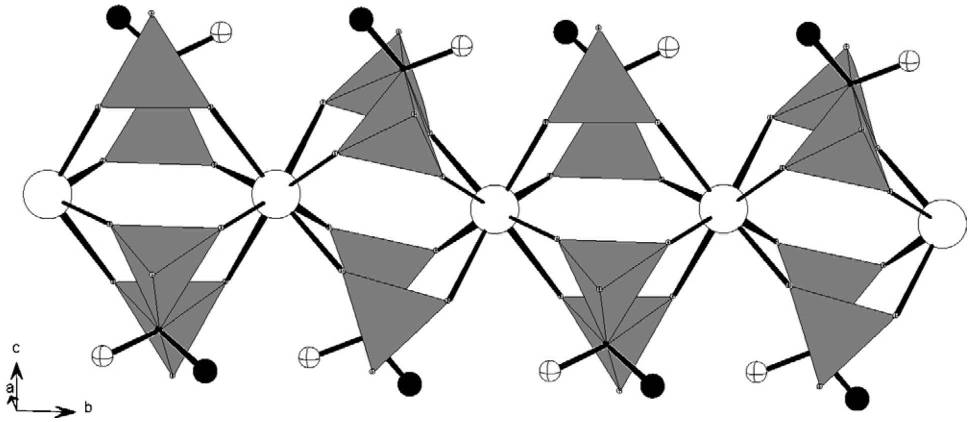

Fig. 12. A 1D lanthanide(III) phosphonate chain in Nd(H_3hedp)(H_2hedp)$_2$·$7H_2O$ (adapted from Ref. [42]).

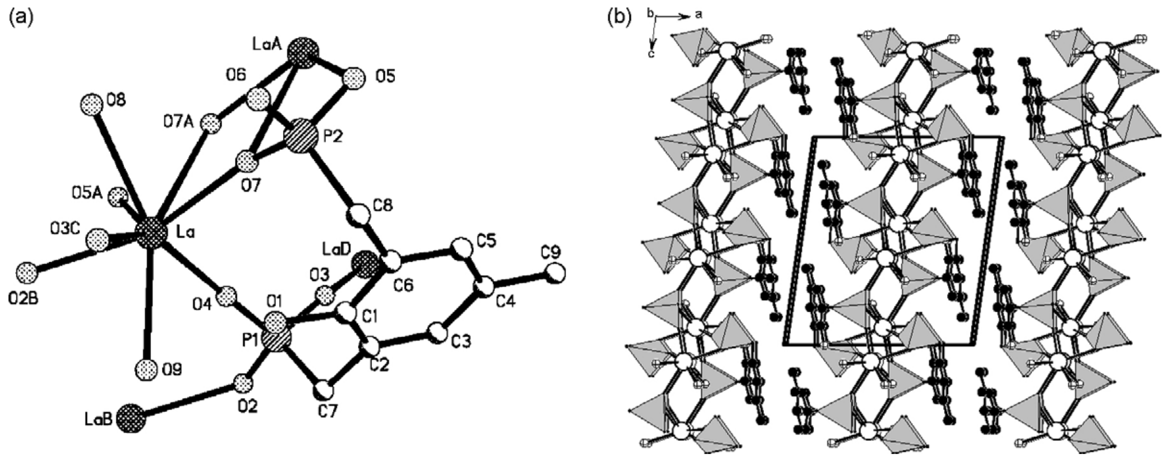

Fig. 14. The selected unit (a) and packing of 2D layers in $La(HL^8)(H_2O)_2$ along *a*-axis (b) (adapted from Ref. [44]).

A few trends can be seen from above discussion. The amine groups of the ligands are usually protonated and remain uncoordinated. The hydroxyl groups are also uncoordinated. Most compounds feature a 1D lanthanide phosphonate chain, such chains can be interconnected into a 2D layer if the phosphonate ligand contains two well separated phosphonate groups. For phosphonic acid with a *N*-oxide group, its lanthanide complexes can be molecular when a stable chelating ring is formed. “Lanthanide contraction” has a strong effect on the deprotonation of the phosphonic acid and the extent of the hydration.

4. Lanthanide complexes with phosphonic acids functionalized with carboxylate groups

Phosphonic acids functionalized with carboxylate groups are versatile ligands since both carboxylate and phosphonate groups are capable of binding with lanthanide(III) ion and these ligands can adopt a variety of coordination modes under different experimental conditions. The structurally characterized lanthanide carboxylate-phosphonates are summarized in Table 3. The first lanthanide phosphonates containing a carboxylate group were reported by Legendziewicz et al. [45,46]. By using *N*-phosphomethylglycine ($H_2O_3PCH_2NHCH_2COOH$), a layered europium(III) complex, $\{Eu_2(HO_3PCH_2NH_2CH_2COO)_2(H_2O)_7(ClO_4)\}[(ClO_4)_3]\cdot H_2O$, was obtained. Its 2D layer is composed of polymeric chains containing two types of dimeric subunits. The first type is created by two 9-coordinate Eu(III) ions bridged by two pairs of carboxylate groups whereas the second type is formed by two 8-coordinate Eu(III) ions bridged by a pair of phosphonate groups. The coordination sphere of the 9-coordinate Eu(III) ion is completed by four aqua ligands whereas that of the 8-coordinate one is satisfied by three aqua ligands and one unidentate perchlorate anion (Fig. 15a). The above two types of dimeric units are interconnected by the organic groups of the amino-carboxylate-phosphonate ligands into a layered architecture (Fig. 15b). The amine group and the phosphonate group are singly protonated. Its emission spectrum exhibits two, five, six and eight lines corresponding to the $^5D_0 \rightarrow {}^7F_j$ transitions (where $j = 0, 1, 2, 4$), which confirms the presence of two types of symmetries for the Eu(III) ions [45].

$Pr[O_3P(CH_2)_2CO_2]$ structurally determined by Serpaggi and Ferey from X-ray powder diffraction data and refined by the Rietveld method [47] features a pillared layered architecture. The praseodymium(III) ion is 7-coordinate with five oxygen atoms from four phosphonate groups and two oxygen atoms from carboxylate groups (Fig. 16a). The phosphonate group is pentadentate, chelating with a Pr(III) ion in a bidentate fashion and also bridging with three other Pr(III) ions. The carboxylate group is bidentate and each oxygen bridges with a Pr(III)

Table 3
Lanthanide complexes of phosphonic acids attached by carboxylate groups

Compound	Structural features	References
$\{Eu_2(HO_3PCH_2NH_2CH_2COO)_2(H_2O)_7(ClO_4)\}[(ClO_4)_3]\cdot H_2O$	Layered	[45,46]
$Pr[O_3P(CH_2)_2CO_2]$	Pillared layered	[47]
$Pr_4(H_2O)_7[O_2C{-}C_5H_{10}N{-}CH_2{-}PO_3]_4\cdot 5H_2O$	3D network	[48]
$La(H_2dpmg)(H_2O)_2\cdot H_2O$	Layered	[49]
$La(H_2dpmg)(H_2O)$	Layered	[49]
$La(H_4L^9)(H_3L^9)(H_2O)\cdot 2H_2O$	Layered	[49]
$Sm(H_2L^9)(H_2O)$	Layered	[50]
$Er(H_3L^9)(H_4L^9)$	1D chain	[49]
$Er(HL^{10})(H_2L^{10})(H_2O)$	Layered	[49]
$[Ln(H_2L^{11})_3]\cdot 2H_2O$ (Ln = Tb, Dy, Eu, Gd)	1D helical chain	[52]
$Ln(HPMIDA)(H_2O)_2\cdot H_2O$ (Ln = Gd, Tb, Dy, Y, Er, Yb, Lu)	3D network with helical tunnels	[53]

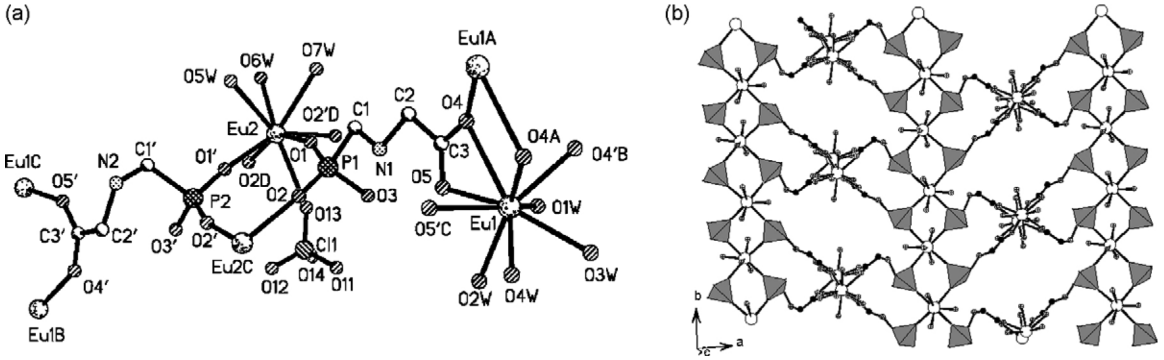

Fig. 15. The selected unit (a) and a 2D lanthanide carboxylate-phosphonate layer (b) in $\{Eu_2(HO_3PCH_2NH_2\ CH_2COO)_2(H_2O)_7(ClO_4)\}[(ClO_4)_3]\cdot H_2O$ (adapted from Ref. [46]).

ion. The interconnection of Pr(III) ions via phosphonate and carboxylate groups resulted in a 2D inorganic layer. Such neighboring layers are further cross-linked by the organic groups of the ligands into a pillared layered structure with an interlayer spacing of ~8.36 Å (Fig. 16b). Isostructural compounds had been prepared for yttrium and the entire series of the lanthanide elements.

Serre et al. reported a new 3D lanthanide complex of a carboxylate phosphonic acid derived from piperidine-4-carboxylic acid ($HO_2C–C_5H_{10}N–CH_2–PO_3H_2$) [48]. The framework of $Pr_4(H_2O)_7[O_2C–C_5H_{10}N–CH_2–PO_3]_4\cdot 5H_2O$ (MIL-84(Pr)) is built up from inorganic chains of edged-sharing PrO_8 or PrO_9 polyhedra and carboxyphosphonate anions, creating a 3D structure with small pores filled with lattice molecules (Fig. 17). Within the inorganic chain, the Pr(III) ions are bridged by phosphonate and carboxylate groups. There are also some unidentate carboxylate groups that complete the coordination sphere of the lanthanide ions. These inorganic chains are interconnected through organic moieties of the carboxylate-phosphonate ligands into a 3D framework with small pores. MIL-84(Pr) is stable up to 523 K with a reversible hydration–dehydration process. Optical studies of its yttrium analogue doped at 3.4% with europium (MIL-84 (Y, Eu)) revealed a significant red-orange emission under UV radiation [48].

The hydrothermal reaction of lanthanum(III) chloride with $(H_2O_3PCH_2)_2NCH_2COOH(H_5dpmg)$ gave a layered compound, $La(H_2dpmg)(H_2O)_2\cdot H_2O$, whereas $La(H_2dpmg)(H_2O)$ with a different layered structure was obtained by using lanthanum(III) hydroxide as the lanthanum source and the reaction was carried out at a little higher temperature [49].

The La(III) ion in $La(H_2dpmg)(H_2O)_2\cdot H_2O$ is 9-coordinate with seven phosphonate oxygen atoms from five $\{H_2dpmg\}^{3-}$ anions and two aqua ligands (Fig. 18a). The La–O distances lie in the range of 2.4453(19) to 2.888(2) Å. The H_2dpmg anion is septadentate. It chelates in a bidentate fashion with one La^{3+} ion by using a phosphonate group and another La(III) ion by using two oxygen atoms from two phosphonate groups, and also bridges with three additional La(III) ions. Two phosphonate oxygen atoms are bidentate bridging. The carboxylate group remains protonated and uncoordinated, so does the amine group. The interconnection of the La^{3+} ions by bridging phosphonate ligands resulted in inorganic layers with the carboxylate moieties

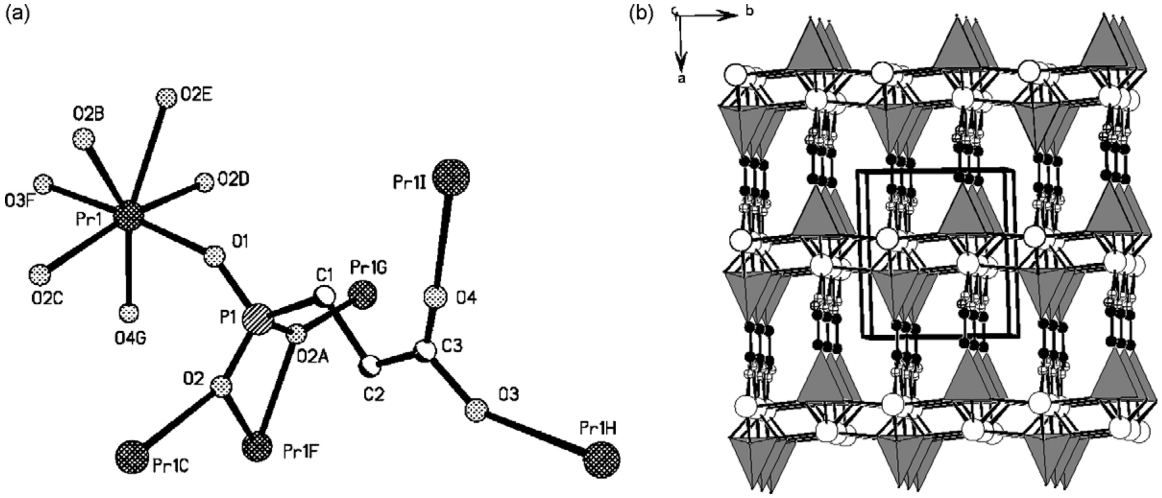

Fig. 16. The selected unit (a) and mixed polyhedral and ball-and-stick projection of the pillared layered structure of $Pr[O_3P(CH_2)_2CO_2]$ along the *c*-axis (b) (adapted from Ref. [47]).

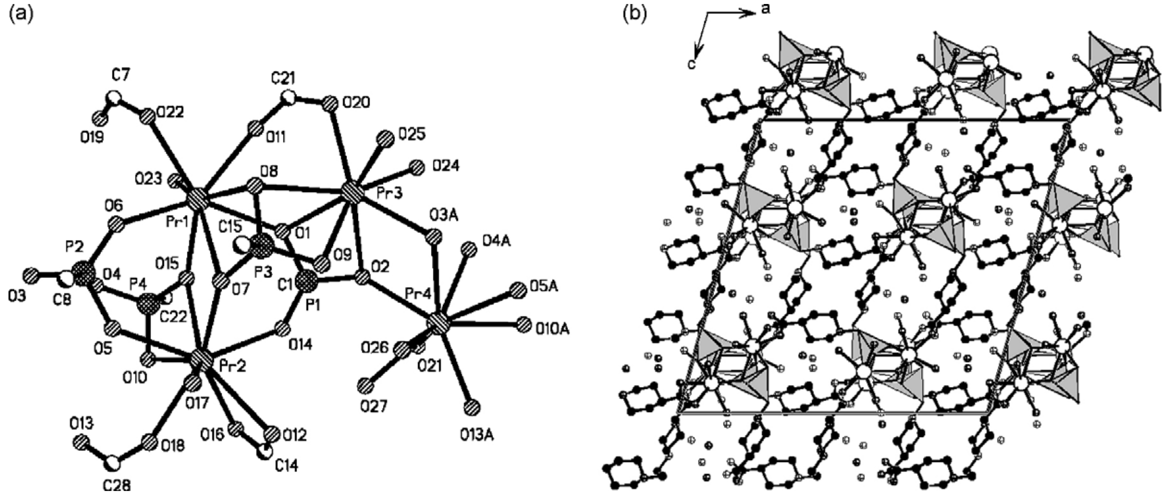

Fig. 17. The coordination geometries around the Pr(III) ions (a) and the structure of $Pr_4(H_2O)_7[O_2C–C_5H_{10}N–CH_2–PO_3]_4·5H_2O$ (b) (adapted from Ref. [48]).

orienting toward the interlayer space (Fig. 18). The interlayer distance is about 12.0 Å. Neighboring layers are held together via hydrogen bonds among carboxylate oxygen atoms, uncoordinated phosphonate oxygen, aqua ligand and lattice water (Fig. 18b).

$La(H_2dpmg)(H_2O)$ exhibits a different layered structure. Its asymmetric unit consists of one unique La^{3+} ion, one $\{H_2dpmg\}^{3-}$ anion and an aqua ligand. The La^{3+} ion is 8-coordinate with five phosphonate oxygen atoms from five phosphonate groups of four $\{H_2dpmg\}^{3-}$ anions, two carboxylate oxygen atoms of another phosphonate ligand and an aqua ligand (Fig. 19a). The La–O distances are in the range of 2.360(9) to 2.728(8) Å. The coordination mode of the phosphonate ligand is different from that in $La(H_2dpmg)(H_2O)_2·H_2O$. One phosphonate group is singly protonated and connects with two La^{3+} ions by using two oxygen atoms. The other phosphonate group is fully deprotonated and bridges with three La^{3+} ions by using three oxygen atoms. The carboxylate group is deprotonated and forms a four-member chelating La–O–C–O ring. The amine group is protonated.

The interconnection of La^{3+} ions via phosphonate ligands led to a double layer (Fig. 19b). The thickness of the double layer is about 9.0 Å. Neighboring 2D layers are held together by weak hydrogen bonds among the amine group, aqua ligand and uncoordinated phosphonate oxygen, as well as weak van der Waals force.

Hydrothermal reactions of lanthanum(III) hydroxide or lanthanide(II) chloride (Ln = Sm, Er) with $4\text{-HOOC–}C_6H_4\text{–}CH_2N(CH_2PO_3H_2)_2(H_5L^9)$ resulted in three new compounds, namely, $La(H_4L^9)(H_3L^9)(H_2O)·2H_2O$, $Sm(H_2L^9)(H_2O)$ and $Er(H_3L^9)(H_4L^9)$ [49,50].

The La^{3+} ion in $La(H_4L^9)(H_3L^9)(H_2O)·2H_2O$ is 7-coordinate with six phosphonate oxygen atoms from five phosphonate ligands and an aqua ligand (Fig. 20a). The La–O distances lie in the range of 2.409(5) to 2.632(7) Å. The $\{H_4L^9\}^-$ anion is bidentate and bridges with two La^{3+} ions, both phosphonate groups are singly protonated, so are the amine group and the carboxylate group. The $\{H_3L^9\}^{2-}$ anion is tetradentate, it forms an eight member chelating ring with a La^{3+} ion, and also bridges with two other La^{3+} ions, one phos-

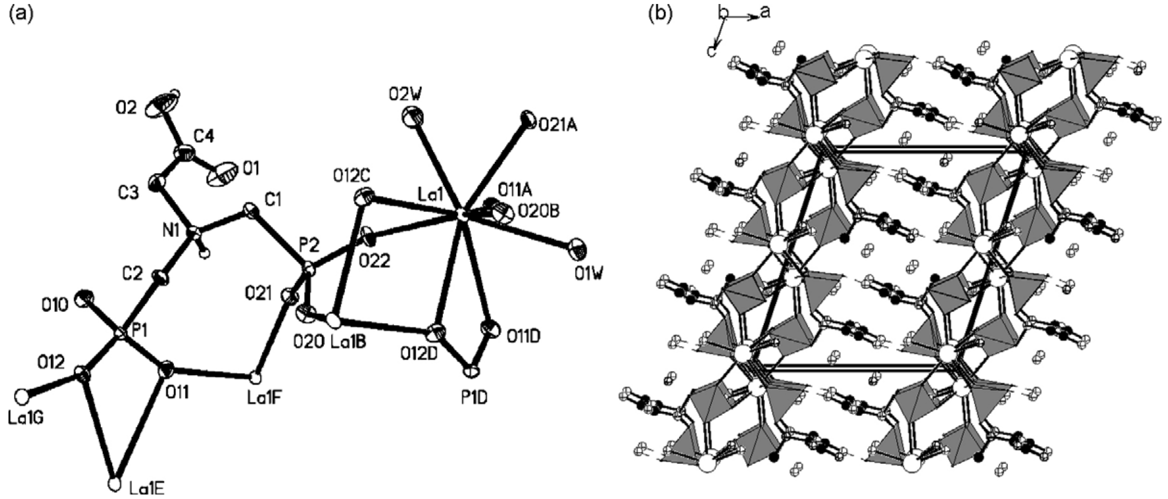

Fig. 18. The selected unit (a) and view of the structure of $La(H_2dpmg)(H_2O)_2·H_2O$ down the *b*-axis (b). Hydrogen bonds are represented by dotted lines (adapted from Ref. [49]).

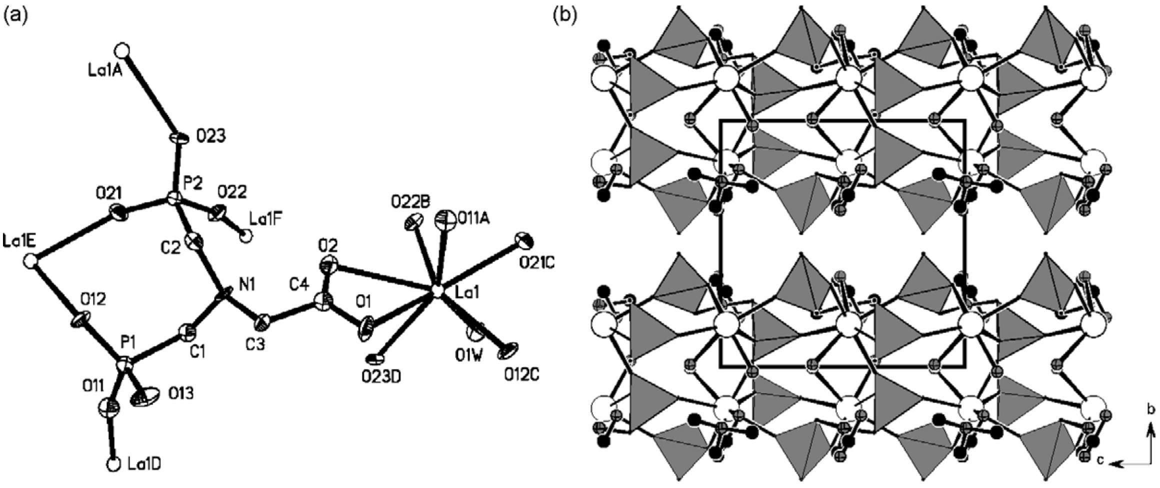

Fig. 19. The selected unit (a) and view of the structure of La(H_2dpmg)(H_2O) down the *a*-axis (b) (adapted from Ref. [49]).

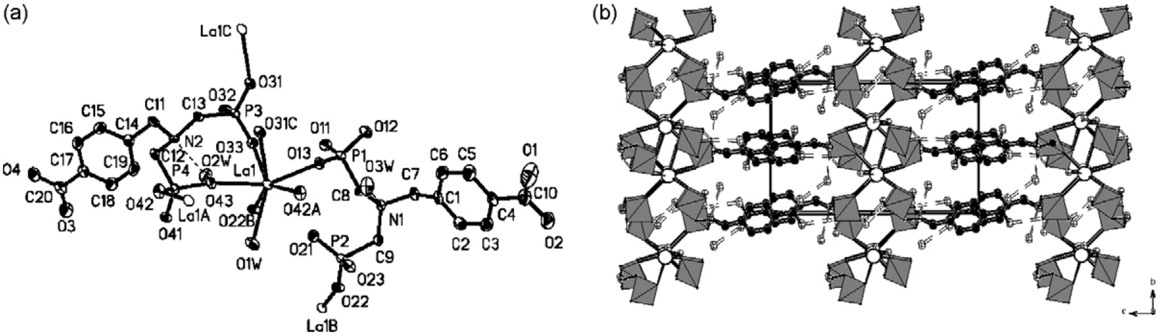

Fig. 20. The selected unit (a) and view of the structure of La(H_4L^9)(H_3L^9)(H_2O)·$2H_2O$ down the *a*-axis (b) (adapted from Ref. [49]).

phonate group is singly protonated and the other one is fully deprotonated, the amine group and the carboxylate group are also protonated.

Adjacent La^{3+} ions are bridged by the above two types of phosphonate anions into a lanthanum phosphonate layer with –C_6H_4–COOH moieties hanging on both sides of the layer (Fig. 20b). Extensive intra-layer and inter-layer hydrogen bonds further cross-link these layers into a 3D supramolecular network. The lattice water molecules are located at the voids of the structure and are involved in hydrogen bonding (Fig. 20). The interlayer distance of about 16.8 Å is significantly larger than that in La(H_2dpmg)(H_2O)$_2$·H_2O, which is due to the additional phenyl group in the phosphonate ligand.

Sm(H_2L^9)(H_2O) features a different layered structure (Fig. 21). The Sm(III) ion is 8-coordinate with seven phosphonate oxygen atoms and an aqua ligand. The phosphonate ligand adopts a different coordination mode. Both phosphonate groups of the $\{H_2L^9\}^{3-}$ anion are fully deprotonated whereas the carboxylate group and the amine group are protonated. One phosphonate group is bidentate bridging with the third oxygen atom uncoordinated. The other phosphonate group is pentadentate, being chelating with a Sm(III) ion and bridging with three

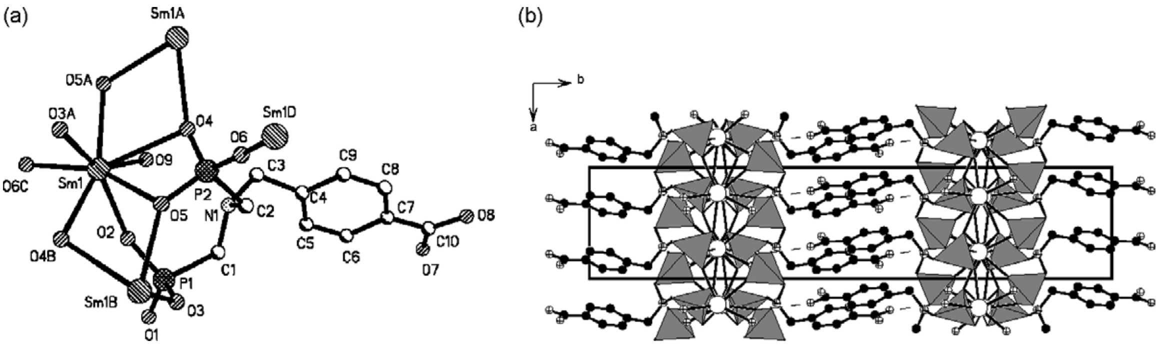

Fig. 21. The selected unit (a) and view of the structure of Sm(H_2L^9)(H_2O) down the *c*-axis (b) (adapted from Ref. [50]).

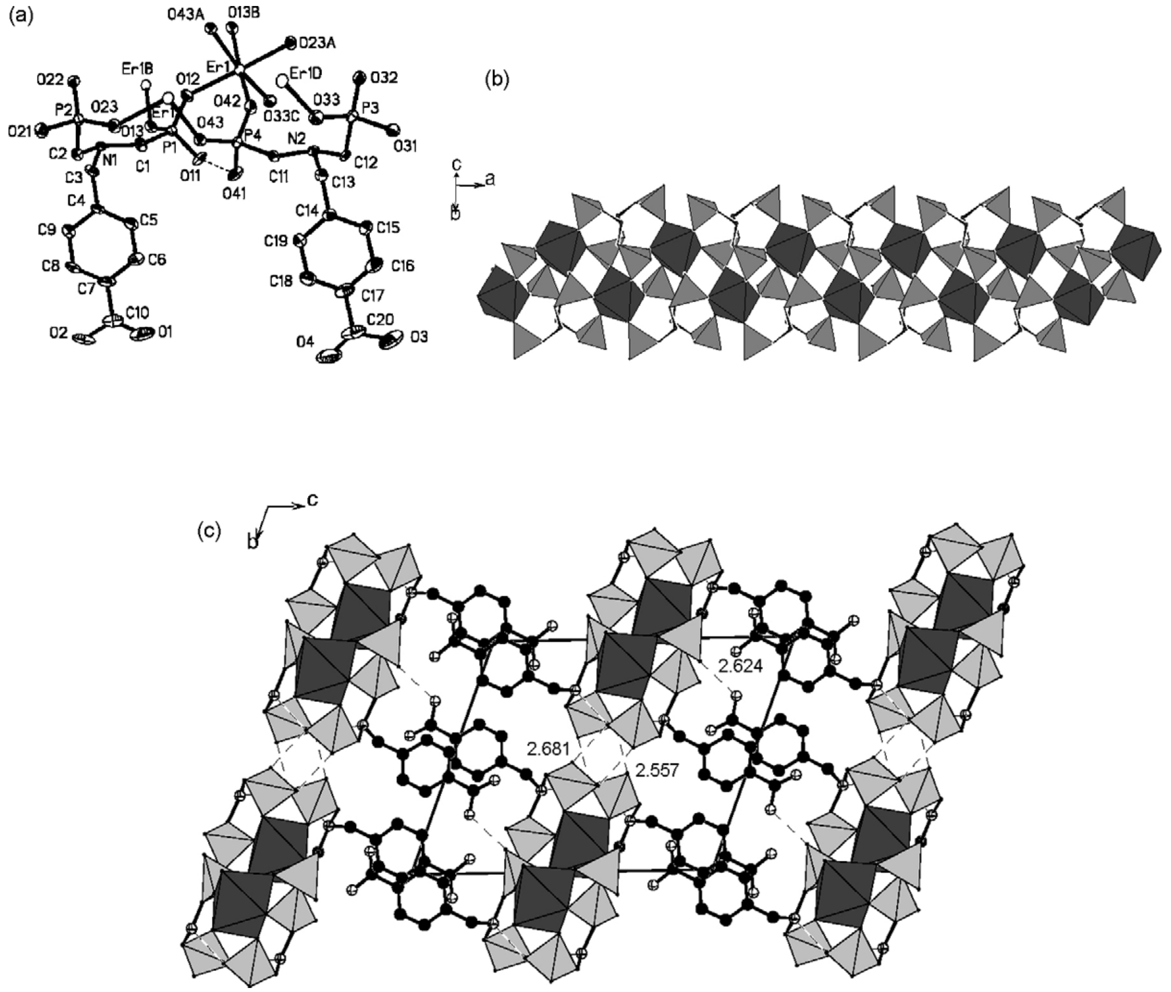

Fig. 22. The selected unit (a), an erbium(III) phosphonate inorganic chain along the *a*-axis (b) and view of the structure of $Er(H_3L^9)(H_4L^9)$ down the *a*-axis (c) (adapted from Ref. [49]).

other Sm(III) ions. The interconnection of Sm(III) ions by the $\{H_2L^9\}^{3-}$ anions resulted in a 2D layer with the carboxylate groups oriented toward the interlayer space. These 2D layers are further cross-linked into a 3D supermolecular network by strong hydrogen bonds formed between the carboxylate groups and the uncoordinated phosphonate oxygen atoms (Fig. 21) [50].

The structure of $Er(H_3L^9)(H_4L^9)$ features a 3D supramolecular network based on 1D erbium(III) phosphonate chains. The Er^{3+} ion is octahedrally coordinate with six phosphonate oxygen atoms from six different phosphonate ligands (Fig. 22a). The coordination modes for the $(H_3L^9)^{2-}$ dianion and $(H_4L^9)^-$ anion are similar. One phosphonate group is monodentate whereas the other is bidentate. The amine group and the carboxylate group in both types of anion are singly protonated. The main difference between the two phosphonate anions is that both phosphonate groups in $(H_4L^9)^-$ anion are singly protonated whereas in $(H_3L^9)^{2-}$ anion only one phosphonate group is singly protonated.

Each pair of Er^{3+} ions are bridged by a pair of phosphonate groups into a 1D chain along the *a*-axis. Such chains are further interconnected via strong hydrogen bonds between uncoordinated phosphonate oxygen atoms into a 2D layer. The $–CH_2–C_6H_4–COOH$ groups of the phosphonate ligands hang in the interlayer space (Fig. 22). The interlayer distance is about 14.3 Å. These 2D layers are further interlinked by hydrogen bonds between carboxylate oxygen and uncoordinated phosphonate oxygen [49].

When erbium(III) nitrate was used as the lanthanide source, $Er(HL^{10})(H_2L^{10})(H_2O)$ was obtained [49]. H_3L^{10} was formed by the *in situ* oxidation of one P–C bond of the H_5L^9 ligand (Scheme 2). Such *in situ* oxidation of the P–C bond has also been observed during the hydrothermal reactions of cobalt(II) nitrate with H_5L^9 [51].

The erbium(III) ion is 7-coordinate with six phosphonate oxygen atoms from five phosphonate ligands and an aqua ligand. The Er–O distances range from 2.214(6) to 2.438(6) Å.

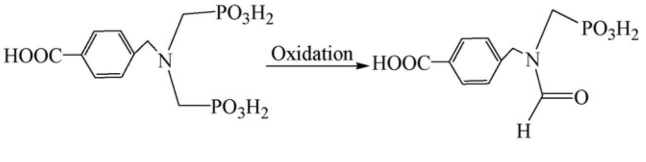

Scheme 2. The formation of H_3L^{10} via the *in situ* oxidation of H_5L^9.

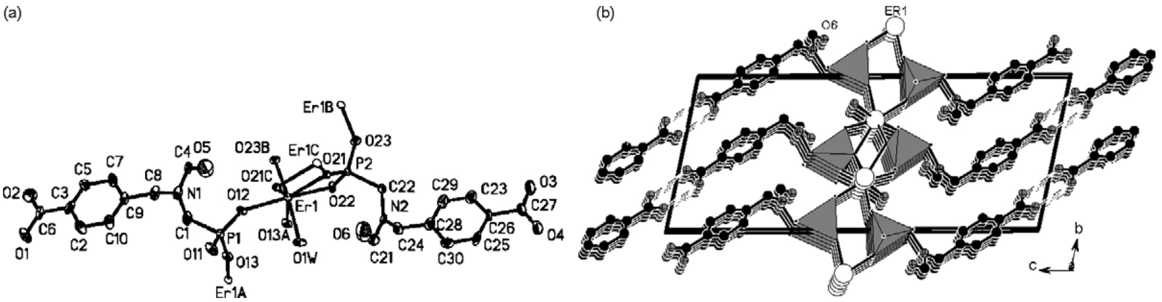

Fig. 23. The selected unit (a) and view of the structure of Er(HL^{10})(H_2L^{10})(H_2O) down the *a*-axis (b) (adapted from Ref. [49]).

The $\{HL^{10}\}^{2-}$ dianion is tetradentate, it forms a chelating ring with an erbium(III) and also bridges with two other erbium(III) ions. The phosphonate group is fully deprotonated whereas the amine group remains protonated. The $\{H_2L^{10}\}^{-}$ anion is bidentate and bridges with two erbium(III) ions by using two oxygen atoms. The third phosphonate oxygen is protonated and uncoordinated, so is the amine group. The carboxylate groups in both types of anions remain uncoordinated. The Er^{3+} ions in Er(HL^{10})(H_2L^{10})(H_2O) are bridged by phosphonate groups of ligands into an inorganic layer (Fig. 23). Neighboring 2D layers are further interlinked via hydrogen bonds between carboxylate groups. The interlayer distance is about 21.6 Å.

The solid-state luminescent properties of Er(H_3L^9)(H_4L^9) and Er(HL^{10})(H_2L^{10})(H_2O) were investigated at room temperature. The emission spectrum of Er(H_3L^9)(H_4L^9) shows three strong near IR emission bands at 1477, 1541 and 1561 nm under 520 nm excitation, all of which were attributed to the $^4I_{13/2} \rightarrow {}^4I_{15/2}$ transition for the Er^{3+} ion. The splitting of the $^4I_{13/2} \rightarrow {}^4I_{15/2}$ transition into several sub-bands is due to the low symmetry of the coordination geometry around the Er^{3+} ion (C_1). The luminescence properties of Er(HL^{10})(H_2L^{10})(H_2O) are very interesting. Surprisingly, Er(HL^{10})(H_2L^{10})(H_2O) shows no near IR emission band under experimental conditions. Under excitation of 408 nm, its emission spectrum exhibits a very broad band with two maximum intensity peaks at 460 and 571 nm, which may be assigned to the intraligand π–π^* fluorescence. The absence of near IR emission was attributed to the quenching effect of the luminescent state by high-frequency vibrating water molecules [49].

Using a chiral phosphonic acid derived from *S*-proline, *S*-HO_3PCH_2–NHC_4H_7–CO_2H(H_3L^{11}), four isostructural homochiral porous lanthanide phosphonates, [Ln(H_2L^{11})$_3$]·$2H_2O$ (Ln = Tb, Dy, Eu, Gd) were synthesized under hydrothermal conditions [52]. These compounds possess a 3D supramolecular framework built up from 1D triple-strand helical chains. Within the helical chain, each Ln(III) ion is octahedrally coordinated with six phosphonate oxygen atoms from six phosphonate ligands and two neighboring Ln(III) ions are bridged by three phosphonate ligands (Fig. 24a). Each phosphonate ligand is bidentate bridging by using two phosphonate oxygen atoms. The third phosphonate oxygen atom and the amine group are protonated and remain uncoordinated. The carboxylate groups of the ligands are also uncoordinated. These uncoordinated functional groups are involved in extensive hydrogen bonding. The helical chains are stacked through hydrogen bonds to form 1D tubular channels along the *c*-axis (Fig. 24b). Moreover, helical water chains are located at the 1D channels. Upon removal of these water chains, the compounds exhibit selective adsorption capacities for N_2, H_2O and CH_3OH molecules. The Tb(III) and Eu(III) compounds exhibit strong green and red fluorescent emissions, respectively, in the solid state at room temperature [52].

By using *N*-(phosphonomethyl)iminodiacetic acid ($H_4PMIDA = H_2O_3PCH_2N(CH_2COOH)_2$), we prepared a series of isostructural chiral lanthanide carboxylate-phosphonates, Ln(HPMIDA)(H_2O)$_2$·H_2O (Ln = Gd, Tb, Dy, Y, Er, Yb, Lu) [53]. The Ln(III) ion is 8-coordinate with a HPMIDA anion in a tetradentate chelating fashion (1N + 3O), one carboxylate and one phosphonate oxygen atom from two other HPMIDA anions as well as two aqua ligands. In addition to chelating with a Ln(III) ion in a tetradentate fashion, the HPMIDA anion also bridges with two other Ln(III) ions. The interconnection of the Ln(III) ions via chelating and bridging HPMIDA anions resulted in a 3D network with chiral tunnels along *a*-axis (Fig. 25). The voids available to the solvent molecules range from 16.0% to 18.0%. TGA studies indicate that the framework remained after removal of the lattice water molecules. Luminescence studies show that the terbium compound exhibits four very strong characteristic emission bands at 490 nm ($^5D_4 \rightarrow {}^7F_6$), 547 nm ($^5D_4 \rightarrow {}^7F_5$), 582 nm ($^5D_4 \rightarrow {}^7F_4$) and 622 nm ($^5D_4 \rightarrow {}^7F_3$) under excitation of 380 nm. The Tb ($^5D_4$) lifetime for $\lambda_{ex,em} = 380$, 488 nm is about 1 ms. The Gd and Er compounds display only very broad ligand-centered (LC) emission bands at 406 and 419 nm, respectively. The absence of emission bands in the near IR region for the Er(III) compound was attributed to the quenching effect of the luminescent state by high-frequency vibrating water molecules [53].

In summary, the attachment of the amino-carboxylic acid moiety to the phosphonic acid can not only improve the solubility and crystallinity of their lanthanide compounds, but also lead to various lanthanide complexes with novel structures and luminescent properties. Most compounds exhibit a layered structure with the amino acid moiety hanging between layers. These uncoordinated carboxylate groups are involved in strong hydrogen bonding. The coordination of carboxylate group usually leads to open framework with higher dimensions.

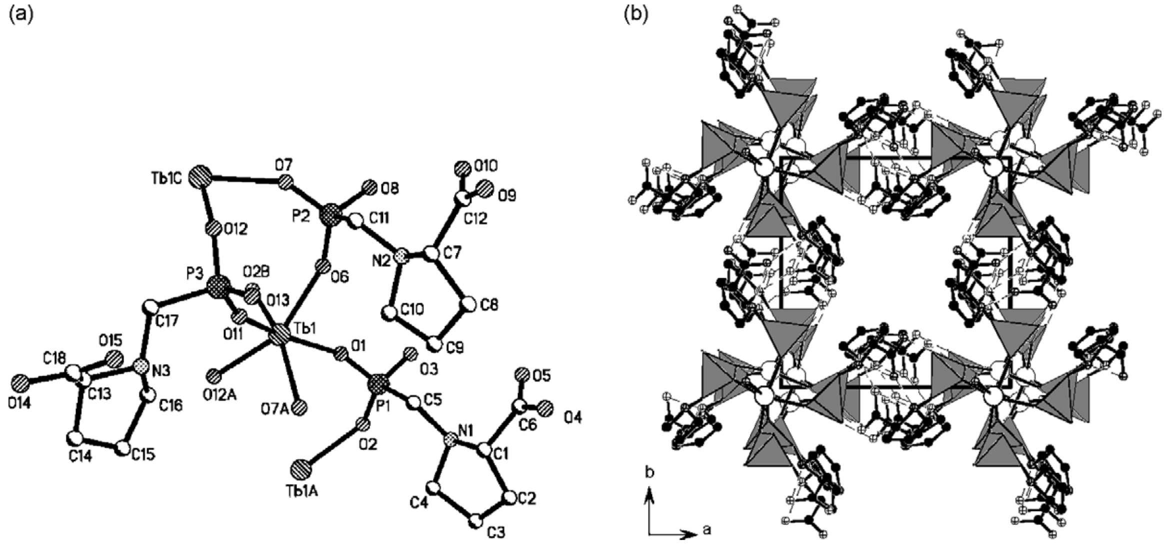

Fig. 24. The selected unit (a) and view of the structure of $[Tb(H_2L^{11})_3]\cdot 2H_2O$ down the *c*-axis (b). The lattice water molecules have been omitted for clarity (adapted from Ref. [52]).

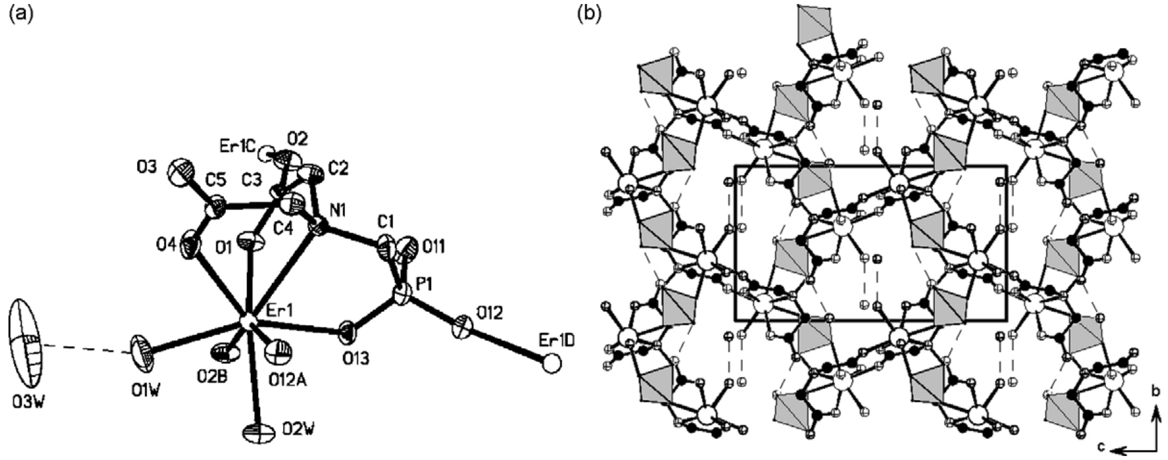

Fig. 25. The selected unit (a) and view of the structure of $Er(HPMIDA)(H_2O)_2\cdot H_2O$ down the *a*-axis (b) (adapted from Ref. [53]).

5. Lanthanide complexes of phosphonic acids attached with macrocyclic moieties

Macrocyclic molecules such as crown ethers, polyaza-crown ethers and calixarenes are good ligands for lanthanide(III) ions, their lanthanide complexes usually have large solubility in water and other organic solvents. Hence their incorporation into the phosphonic acids can greatly improve the solubility and crystallinity of the lanthanide phosphonates formed. Furthermore, besides providing additional coordination atoms for the lanthanide(III) ions, the crown moiety can also act as the host molecules for many types of guest molecules such as organic solvents. Lanthanide complexes of phosphonic acids attached with a macrocyclic moiety are summarized in Table 4.

Clearfield et al. reported the first lanthanide complex of phosphonic acid derived from aza-12-crown ether-4, $Ce(NO_3)_3(H_2O)_2(HO_3PCH_2NHC_{10}H_{20}O_4)$ [54]. The cerium(III) compound forms a dimer by covalent bonding to two phosphonate groups that bridge across the Ce. The 10-fold coordination of the cerium atoms is completed by means of three bidentate nitrate ions and two water molecules. The phosphonate ligand is neutral, and both the phosphonate group and the amine group are singly protonated. The dimers then form hydrogen bonds to each other, via water as donors and nitrate oxygen atoms as acceptors (O···O 2.698(5), 2.772(5) Å), forming linear chains as illustrated in Fig. 26.

Ngo and Lin designed a diphosphonic acid based on chiral crown ether (H_4L^{12}) and isolated two lanthanide complexes, $[Ln_2(HL^{12})_2(MeOH)_8]\cdot H_4L^{12}\cdot 3HCl\cdot 6H_2O$ (Ln = Nd, Sm) [55]. There exists two types of phosphonate ligands, one is 1H-protonated and the other is neutral. The lanthanide(III) ions are 8-coordinate with four phosphonate oxygen atoms from four phosphonate ligands and four methanol solvents. Both phosphonate groups of the 1H-protonated ligand adopt a bidentate bridging coordination mode. The interconnection of Ln(III) ions via bridging ligands resulted in a layered architecture. The crown

Table 4
Lanthanide complexes of phosphonic acids derived from macrocyclic molecules

Compound	Structural features	Reference
$Ce(NO_3)_3(H_2O)_2(HO_3PCH_2NHC_{10}H_{20}O_4)$	Dimer	[54]
$[Ln_2(HL^{12})_2(MeOH)_8]\cdot H_4L^{12}\cdot 3HCl\cdot 6H_2O$ (Ln = Nd, Sm)	Layered	[55]
$[Ln(H_2L^{13})(NO_3)(H_2O)_2]\cdot 2H_2O\cdot 2MeOH$ (Ln = La, Pr, Nd)	Porous 3D network	[56]
$Li[Nd(Hdo3ap)(H_2O)]\cdot 11.5H_2O$	1D chain	[57]
$Li[Tb(Hdo3ap)(H_2O)]\cdot 0.5HCl\cdot 5H_2O$	1D chain	[58]
$Li[Ln(Hdo3ap)]\cdot 5H_2O$ (Ln = Dy, Y, Lu)	Isolated	[58]
$H[Ln(Hdo3ap)]\cdot xH_2O$ (Ln = Er, x = 5; Ln = Lu, x = 6)	Isolated	[58]
$La(H_5L^{14})$	Isolated	[59]
$[\{Na_{13}(OH)_3(H_2O)_{29}\}\{Gd(DOTP)\}][Gd(DOTP)]\cdot 7H_2O\cdot 2CH_3CH_2OH$	Layered	[60]

ether moieties of the ligands remain uncoordinated and are oriented toward the interlayer space. The neutral phosphonate ligands are also located at the interlayer space (Fig. 27). The layered structure is retained after the removal of guest molecules. Such chiral crown ether groups between lanthanide phosphonate layers have the potential to enantioselectively interact with organic cations such as protonated amino acids and thereby provide a novel material for bulk chiral separation if the porosity of such material is large enough [55].

By using 25,27-dimethoxy-26, 28-dihydroxycalix[4]arene-11, 23-diphosphonic acid (H_4L^{13}), Lukeš and coworkers isolated a series of lanthanide complexes generally formulated as $[Ln(H_2L^{13})(NO_3)(H_2O)_2]\cdot 2H_2O\cdot 2MeOH$ (Ln = La, Pr, Nd) [56]. These compounds are unstable when removed from their mother liquids, and lose the methanol molecules under atmospheric conditions. The structures of these compounds feature an interesting 3D network with large pores (Fig. 28). Each of the *cone* shaped molecules of the diphosphonic acid serves as a tetradentate bridging ligand, connecting with four Nd(III) atoms. Four of these Nd–calixarene–Nd units are interconnected into the supramolecular ring. These rings are connected to the 2D net and through the O–P–O bridges in the third dimension forming porous 3D polymeric structure (Fig. 28). The pores are approximately 17 Å in diameter. These, mainly hydrophobic, tubules were thought to be available for larger amphiphilic organic molecules encapsulation [56].

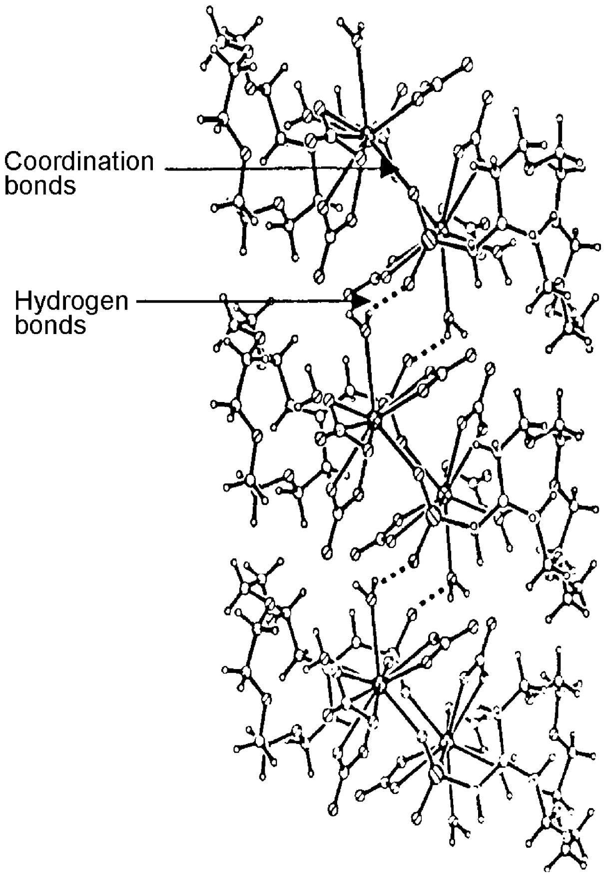

Fig. 26. The 1D polymeric hydrogen bonded chain based on dimer units in $Ce(NO_3)_3(H_2O)_2(HO_3PCH_2NHC_{10}H_{20}O_4)$ (adapted from Ref. [54]).

Lukeš and coworkers also reported a series of lanthanide complexes with 1,4,7,10-tetraazacyclodecane–1,4,7-triacetic–10-methylphosphonic acid (H_5do3ap), $M[Ln(Hdo3ap)]\cdot xH_2O$ (M = Li or H and Ln = Nd, Tb, Dy, Er, Lu and Y) [57,58]. The lanthanide ions in all these compounds form a $\{Ln(Hdo3ap)\}^-$ chelating unit by using 4 O and 4 N atoms from a Hdo3ap ligand. The connectivity between the $\{Ln(Hdo3ap)\}^-$ chelating units is different. In $Li[Nd(Hdo3ap)(H_2O)]\cdot 11.5H_2O$, the Li(I) ion is tetrahedrally coordinate with one phosphonate and one carboxylate atoms from two chelating units as well as two aqua ligands. The bridging of the $\{Nd(Hdo3ap)\}^-$ chelating units via Li(I) cations resulted in a 1D chain along *a*-axis (Fig. 29a). In $Li[Tb(Hdo3ap)(H_2O)]\cdot 0.5HCl\cdot 5H_2O$, the Li(I) ion is tetrahedrally coordinated with one carboxylate and two phosphonate atoms from two $\{Tb(Hdo3ap)\}^-$ chelating units as well as an aqua ligand. Neighboring $\{Tb(Hdo3ap)\}^-$ chelating units are bridged by Li(I) ions (O (phosphonate)–Li–O(phosphonate)) into a 1D zigzag chain along *b*-axis (Fig. 29b). In $Li[Ln(Hdo3ap)]\cdot 5H_2O$ (Ln = Dy, Y, Lu), the Li(I) cation connects with only one chelating unit due to the coordination of three aqua ligands (Fig. 29c). When the Li(I) ion is replaced by a proton, neighboring [Ln(Hdo3ap)] units are interconnected only via hydrogen bonds among uncoordinated carboxylate and phosphonate oxygen atoms as well as lattice water molecules.

Bligh et al. synthesized a phosphonic acid containing four methylenephosphonate pendant arms based on 18-membered hexaaza macrocycle (H_8L^{14}) and its lanthanum complex $La(H_5L^{14})$ [59]. The lanthanum(III) ion is 10-coordinate with six nitrogen atoms of the crown ring and four oxygen atoms from four pendant arms. The six nitrogen atoms are almost coplanar

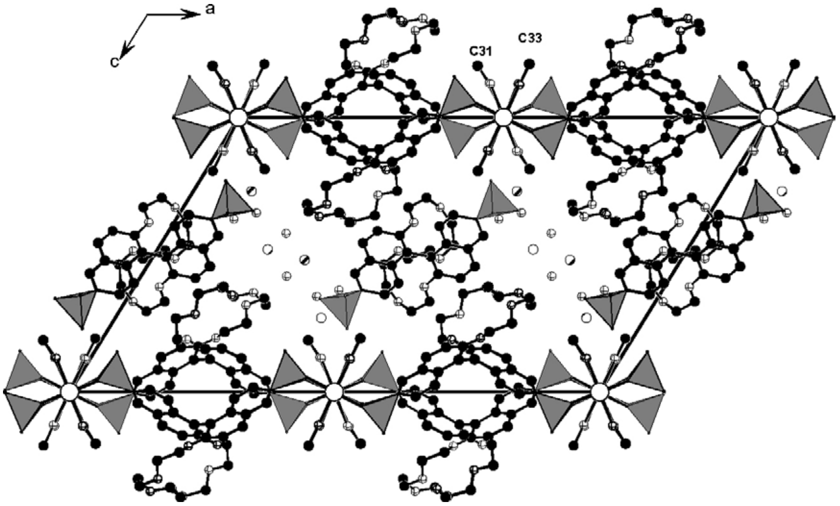

Fig. 27. View of structure of $[Ln_2(HL^{12})_2(MeOH)_8]\cdot H_4L^{12}\cdot 3HCl\cdot 6H_2O$ (Ln = Nd, Sm) down the *b*-axis (adapted from Ref. [55]).

with the lanthanum(III) ion whereas the four pendant arms are located at both sides of the plane. Four protons may be assigned to the four longest bonds [range 1.558–1.587(9) Å] and it seems that the fifth one is probably disordered over the rather shorter two P–O bonds (1.526–1.534 Å). The $La(H_5L^{14})$ chelating units are interlinked via hydrogen bonds between uncoordinated phosphonate oxygen atoms into a 2D supermolecular architecture (Fig. 30).

A sodium-lanthanide complex of 1,4,7,10-tetraazacyclododecane–1,4,7,10-tetrakis(methylenephosphonic acid) (H_8DOTP), $[\{Na_{13}(OH)_3(H_2O)_{29}\}\ \{Gd(DOTP)\}][Gd(DOTP)]\cdot 7H_2O\cdot 2CH_3CH_2OH$, was reported by Geraldes and coworkers [60]. There are two unique Gd(III) ions in the structure, each is octadentate, chelated by a DOTP anion. The first-type of {Gd(DOTP)} anions connect with the sodium clusters directly by using its four phosphonate oxygen atoms, resulting in a 2D layer with the isolated {Gd(DOTP)} anions (second type) located at interlayer space (Fig. 31). This type of lanthanide compound may be used as a paramagnetic shift reagent for the *in vivo* NMR spectroscopy of cations and as contrast agents for magnetic resonance imaging (MRI).

In summary, lanthanide complexes with phosphonic acids derived from polyaza-crown ethers generally feature a molecular structure in which the lanthanide cation is encapsulated by the crown moiety, these molecular units are further interconnected into a supermolecular architecture through strong hydrogen bonds between uncoordinated phosphonate oxygen atoms from neighboring chelating units. If one proton of the unit is replaced by a Li^+ ion, these molecular units could possibly be interconnected into a 1D array through bridging Li^+ ions. The oxygen atoms of a crown ether ring or a calixarene are usually much weaker donors than those of the phosphonate groups, hence such a crown ring remains uncoordinated and can encapsulate various guest molecules such as lattice water molecules or organic solvents.

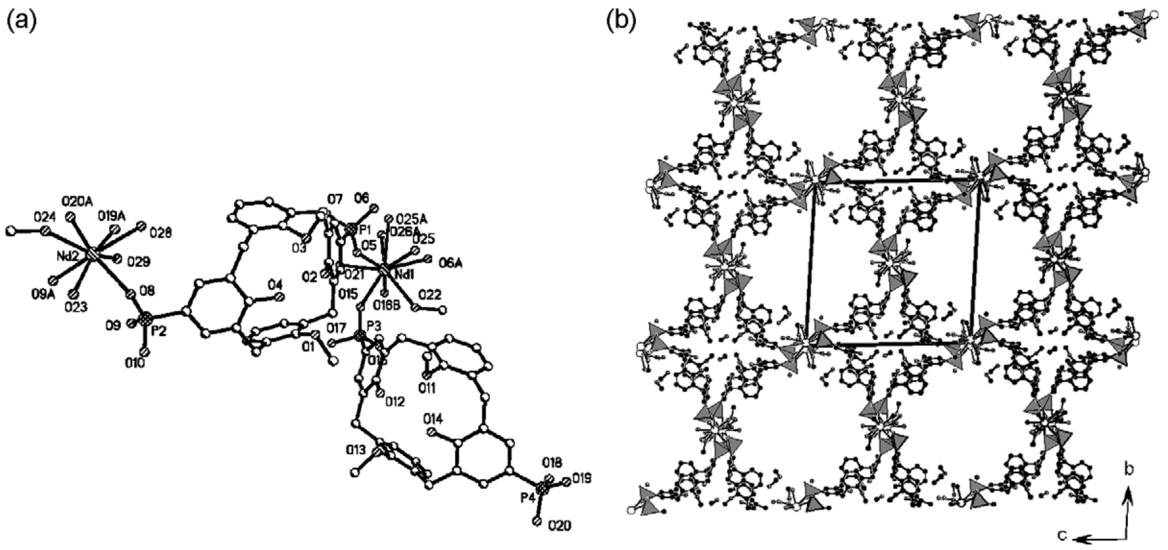

Fig. 28. The selected unit (a) and view of structure of $[Nd(H_2L^{13})(NO_3)(H_2O)_2]\cdot 2H_2O\cdot 2MeOH$ down the *a*-axis (b) (adapted from Ref. [56]).

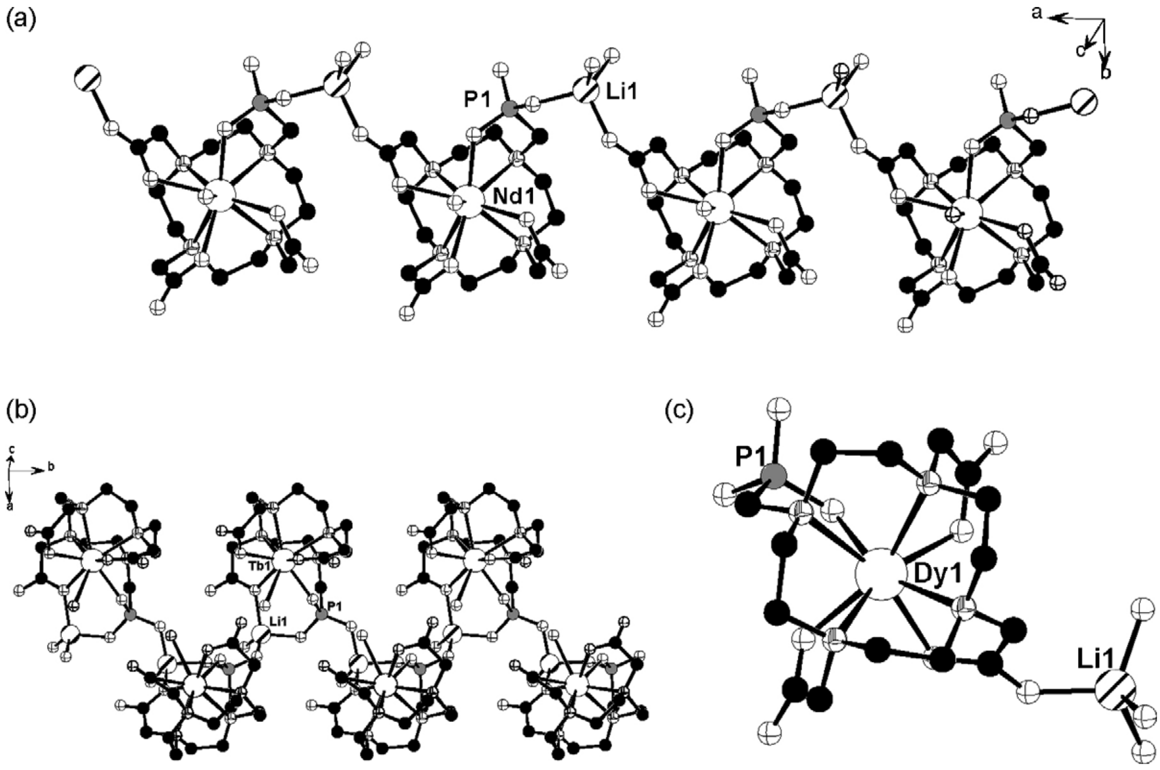

Fig. 29. Connectivity between the Ln(Hdo3ap) chelating units in the Nd (a), Tb (b) and Dy (c) complexes (adapted from Ref. [57,58]).

6. Lanthanide phosphonates containing a second metal linker

As mentioned earlier, another alternative method to solve the solubility and crystallinity problems is to introduce a second metal linker. These lanthanide compounds have large solubility in water and better crystallinity. A list of lanthanide phosphonates containing a second metal linker is summarized in Table 5.

Hydrothermal reactions of lanthanide metal salts with $MeN(CH_2CO_2H)(CH_2PO_3H_2)(H_3L^{15})$ and 5-sulfoisophthalic acid monosodium salt (NaH_2BTS) lead to a serious of layered lanthanide carboxylate-phosphonate-sulfonate hybrids, namely,

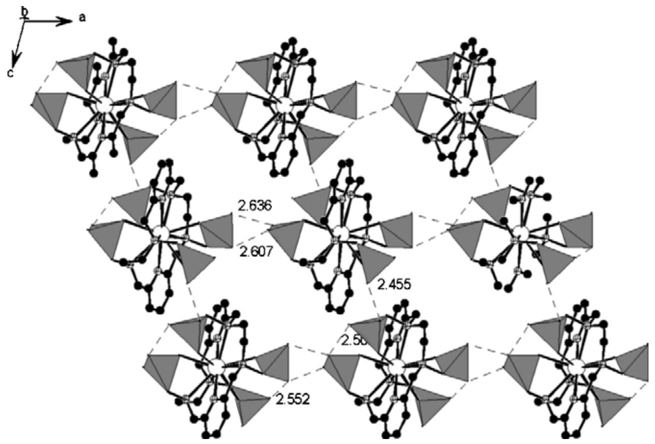

Fig. 30. Part of the 2D hydrogen-bonded network in the solid-state structure of $[La(H_5L^{14})]$ (adapted from Ref. [59]).

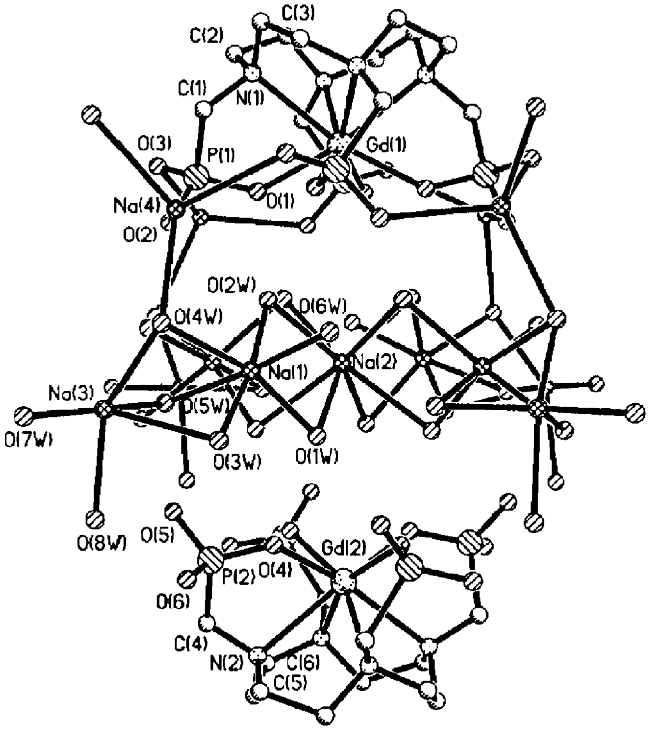

Fig. 31. A general view of the super molecule in the solid state, including the external spheres of the $[Gd(1)(DOTP)]^{5-}$ and $[Gd(2)(DOTP)]^{5-}$ moieties (adapted from Ref. [60]).

Table 5
Lanthanide phosphonates containing a second metal linker

Compound	Structural features	Reference
$Ln(H_2L^{15})(HBTS)(H_2O)_2{\cdot}H_2O$ (Ln = La, Pr, Nd and Gd)	Layered	[61]
$Ln(C_2O_4)\{H_2L^{15}\}{\cdot}0.5H_2O$ (Ln = Nd, Eu, Gd)	3D network	[62]
$Ln_4(C_2O_4)_5(HL^{16})_2(H_2O)_4{\cdot}2H_2O$ (Ln = La, Nd)	3D network	[62]
$Ln_3(C_2O_4)_4(HL^{16})(H_2O)_6{\cdot}6H_2O$ (Gd, Er)	3D network	[62]
$La_2(ox)_2(H_6L^7){\cdot}2H_2O$	3D network	[63]
$Ln_2(ox)_2(H_6L^7)(H_2O)_2{\cdot}4H_2O$ (Ln = Nd, Eu)	3D network	[63]
$[La_2(L^{17})_2(phen)_4(H_2O)]{\cdot}4.5H_2O$	1D cluster chain	[64]
$[Ln_2(L^{17})_2(phen)_2(H_2O)_5]{\cdot}3H_2O$ (Ln = Nd, Eu, Er)	Tetranuclear cluster	[64]
$[Ln_2(HL^{17})(H_2L^2)_2(H_2O)_4]{\cdot}8H_2O$ (Ln = La, Nd)	3D cluster network	[64]

$Ln(H_2L^{15})(HBTS)(H_2O)_2{\cdot}H_2O$ (Ln = La, Pr, Nd and Gd) [61]. The asymmetric unit of these isostructural compounds is composed of one Ln(III) ion, one $(H_2L^{15})^-$ anion, one HBTS anion, two aqua ligands and a lattice water molecule (Fig. 32a). The lanthanide ion is 9-coordinate with three carboxylate oxygen atoms from two $(H_2L^{15})^-$ anions, two phosphonate oxygen atoms from two other $(H_2L^{15})^-$ anions, one carboxylate oxygen atom from a $HBTS^{2-}$ anion and one sulfonate oxygen atom from another $HBTS^{2-}$ anion as well as two aqua ligands. The $(H_2L^{15})^-$ anion is pentadentate, it chelates with one lanthanide ion in a bidentate fashion by using its carboxylate group and bridges with four other lanthanide centers. One carboxylate oxygen acts as a μ_2-metal linker. Two phosphonate oxygen atoms are unidentate, whereas the third one is protonated and uncoordinated. The amine group is also protonated and uncoordinated. The $HBTS^{2-}$ anion is bidentate and bridges with two lanthanide ions by using a sulfonate and a carboxylate oxygen atoms. The second carboxylate group of $HBTS^{2-}$ anion is protonated and uncoordinated. The interconnection of Nd(III) atom by the carboxylate phosphonate $\{H_2L^{15}\}^-$ anions resulted in a $Nd_2(HL^{15})_2$ unit, and such neighboring unit is bridged by the carboxylate groups to form a 1D double chain along the *a*-axis. These double chains are cross-linked by bridging HBTS anions to form a lanthanide phosphonate-sulfonate hybrid layer (Fig. 32b). The lattice water molecule is hydrogen bonded to the aqua ligand and the amine group. The uncoordinated phosphonate oxygen also forms hydrogen bonds with uncoordinated carboxylate oxygen atoms of the HBTS anion [61].

Upon complexion of both ligands with the lanthanide(III) ions, the luminescent spectra of the compounds formed exhibit emission bands characteristic of the corresponding lanthanide(III) ions. Upon excitation at 310 nm, the neodymium(III) compound displays a strong blue fluorescent emission band at 410 nm ($^4D_{3/2} \rightarrow {}^4I_{13/2}$ transition). Under excitation of 356 nm the neodymium(III) compound displays a strong emission band at 902 ($^4F_{3/2} \rightarrow {}^4I_{9/2}$), an emission band with much lower intensity at 1067 nm ($^4F_{3/2} \rightarrow {}^4I_{11/2}$) and a very weak band at 1338 nm ($^4F_{3/2} \rightarrow {}^4I_{13/2}$) in the near IR region. The spectrum of gadolinium(III) compound only shows a strong fluorescent emission band at 416 nm ($\lambda_{ex} = 318$ nm). Upon removal of the lattice water and two aqua ligands, the emission band at 410 nm of Nd(III) compound disappeared whereas other emission bands are slightly shifted to lower wavelengths and their intensities enhanced greatly. The emission band for Gd(III) compound was shifted to 464 nm and its intensity is also significantly enhanced after dehydration [61].

When oxalate anion was used as the second metal linker instead of 5-sulfoisophthalic acid, a serious of novel lanthanide oxalate phosphonate hybrids with 3D network structures were obtained, namely, $Ln(C_2O_4)\{H_2L^{15}\}{\cdot}0.5H_2O$ (Ln = Nd, Eu, Gd) [62]. The structure of these isomorphous lanthanide compounds feature a 3D network formed by 3D $\{Ln(H_2L^{15})\}^{2+}$

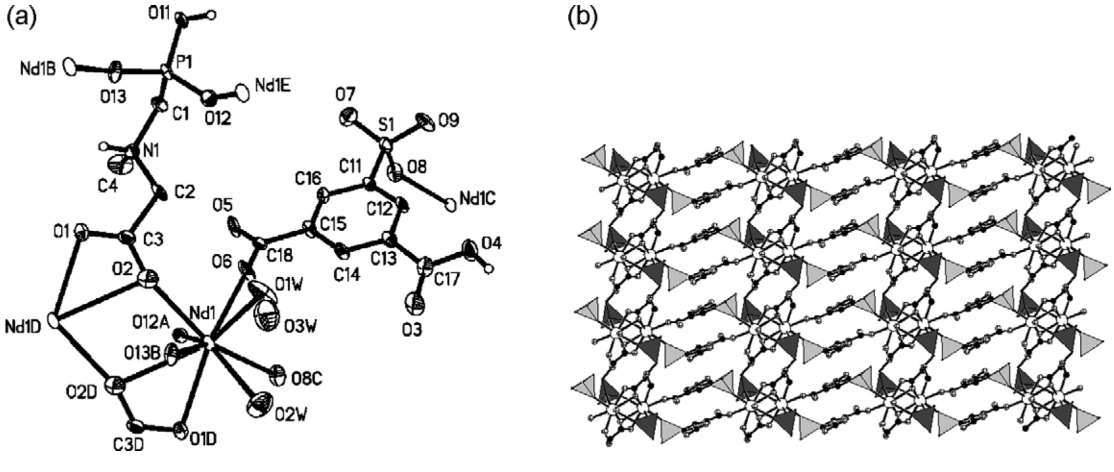

Fig. 32. The selected unit (a) and the layered architecture of the $Nd(H_2L^{15})(HBTS)(H_2O)_2{\cdot}H_2O$. The phosphonate and sulfonate tetrahedra are shaded in heavy and light gray, respectively (adapted from Ref. [61]).

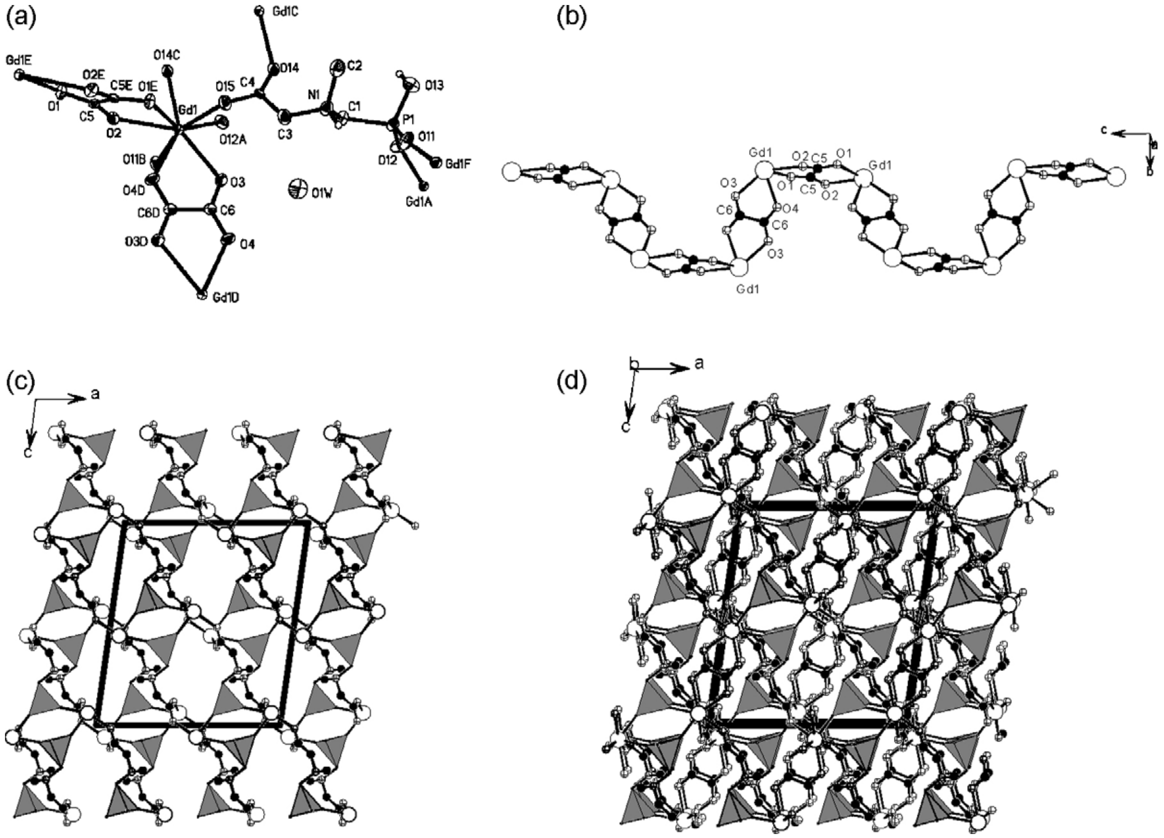

Fig. 33. The selected unit of $\{Gd(C_2O_4)(H_2L^{15})\}\cdot 0.5H_2O$ (a), a 1D helix chain of $\{Gd(C_2O_4)\}^+$ (b) and a 3D network of $\{Gd(H_2L^{15})^{2+}$ (c), and a view of the structure of $\{Gd(C_2O_4)(H_2L^{15})\}\cdot 0.5H_2O$ down the *b*-axis (d) (adapted from Ref. [62]).

and 1D $\{Ln(C_2O_4)\}^+$ cations. The Ln(III) ion is 8-coordinate with four oxygen atoms from two oxalate anions, two carboxylate and two phosphonate oxygen atoms from four $(H_2L^{15})^-$ anions (Fig. 33a). Each oxalate anion is tetradentate and forms two Ln–O–C–C–O five-member chelating rings. The $(H_2L^{15})^-$ anion is tetradentate and bridges with four Ln(III) ions. The interconnection of Ln(III) by chelating and bridging oxalate anions results in a 1D helical chain of $\{Ln(C_2O_4)\}^+$ (Fig. 33b). The cross-linkage of Ln(III) ions by bridging $(H_2L^{15})^-$ anions lead to a 3D network with tunnels along *b*-axis (Fig. 33c). The above two building units are interconnected via sharing Ln(III) ions to form a complex 3D network (Fig. 33d). The structure of this series of compounds can also be viewed as the oxalate anions occupying the tunnels of the 3D network of $\{Ln(H_2L^{15})\}^{2+}$. Luminescence studies indicate that the Nd(III) compound exhibit several emission bands in the near IR region, the Gd(III) complex displays a broad blue fluorescent emission band at 451 nm and the Eu(III) compound shows very strong and sharp emission bands at 592, 616 and 699 nm with a long luminescent lifetime of 1.13 ms [62].

The use of $Me_2NCH_2PO_3H_2(H_2L^{16})$ in the syntheses afforded two different series of new lanthanide oxalate phosphonates, namely, $Ln_4(C_2O_4)_5(HL^{16})_2(H_2O)_4\cdot 2H_2O$ (Ln = La, Nd) and $Ln_3(C_2O_4)_4(HL^{16})(H_2O)_6\cdot 6H_2O$ (Gd, Er) [62].

Among two unique Ln(III) ions in the asymmetric unit of $Ln_4(C_2O_4)_5(HL^{16})_2(H_2O)_4\cdot 2H_2O$ (Ln = La, Nd), one is 8-coordinate with six oxygen atoms from four oxalate anions, one phosphonate oxygen from one $\{HL^{16}\}^-$ anion and an aqua ligand, whereas the other one is 9-coordinate with five oxygen atoms from three oxalate anions, three phosphonate oxygen atoms from two $\{HL^{16}\}^-$ anions as well as an aqua ligand (Fig. 34a). The $\{HL^{16}\}^-$ anion is tetradentate, chelating with one Ln(III) ion in a bidentate fashion and also bridging with two other Ln(III) ions. One phosphonate oxygen is μ_2-bridging, whereas the other two are unidentate. There are two different coordination modes for the five oxalate anions in the formula unit. One oxalate anion is hexadentate. It forms two chelating rings with two Ln(III) ions and also bridges with two other lanthanide ions. The remaining four oxalate anions are tetradentate.

The interconnection of Ln(III) atoms by bridging and chelating $\{HL^{16}\}^-$ anions results in a $Ln_4(HL^{16})_2$ unit, in which two Ln(III) atoms are bridged by a pair of phosphonate groups to form a dimeric unit, and such a dimeric unit further connects with two other Ln(III) atoms through μ^2-phosphonate oxygen atoms. The interconnection of Ln(III) ions by chelating and bridging oxalate anions lead to a 3D network of $\{Ln_4(C_2O_4)_5\}^{2+}$ with tunnels running along *c*-axis. The tunnel is formed by 24 member rings composed of six Ln(III) ions and six oxalate anions (Fig. 34b). The above two types of building blocks are interconnected into a 3D network (Fig. 34c). The structure of $Ln_4(C_2O_4)_5(HL^{16})_2(H_2O)_4\cdot 2H_2O$ (Ln = La, Nd) can also be viewed as the $\{HL^{16}\}^-$ anions being inserted in the tunnels of $\{Ln_4(C_2O_4)_5\}^{2+}$. Under excitation of 826 nm, the Nd(III) compound displays the characteristic emission bands for the Nd(III)

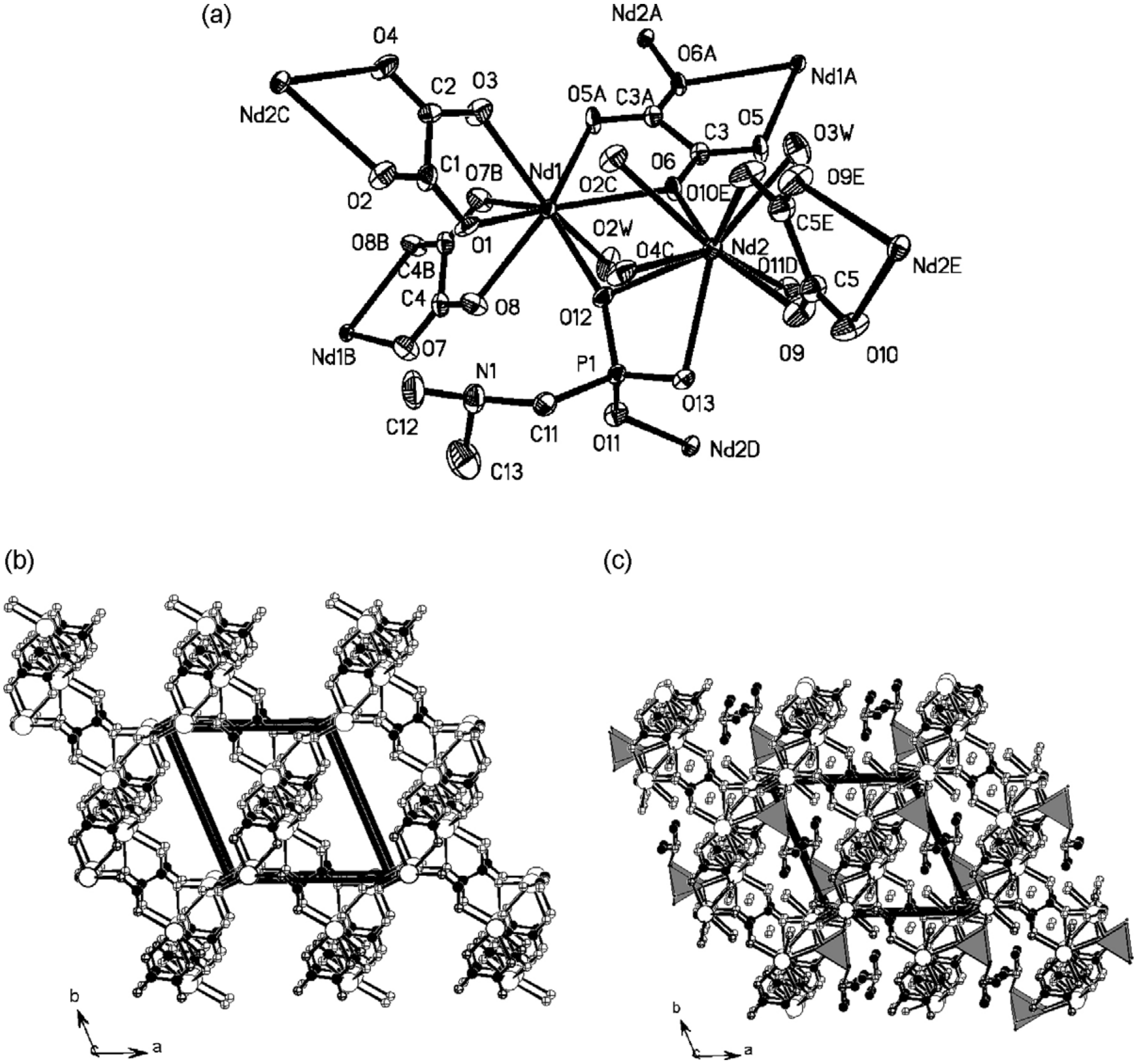

Fig. 34. The selected unit in $Nd_4(C_2O_4)_5(HL^{16})_2(H_2O)_4\cdot 2H_2O$ (a), the 3D network of $\{Nd_4(C_2O_4)_5\}^{2+}$ (a) and view of the structure of $Nd_4(C_2O_4)_5(HL^{16})_2(H_2O)_4\cdot 2H_2O$ down the *c*-axis (c) (adapted from Ref. [62]).

ion: a weak emission band at 896 nm ($^4F_{3/2} \rightarrow I_{9/2}$), a strong emission band at 1063 nm ($^4F_{3/2} \rightarrow {}^4I_{11/2}$) and a very weak band at 1388 nm ($^4F_{3/2} \rightarrow {}^4I_{13/2}$) in the near IR region. The Nd ($^4F_{3/2}$) lifetimes were measured to be 18.7 μs [62].

The heavier lanthanide(III) complexes form a different type of 3D network, $Ln_3(C_2O_4)_4(HL^{16})(H_2O)_6\cdot 6H_2O$ (Gd, Er). There are three unique Ln(III) ions in the asymmetric unit of $Ln_3(C_2O_4)_4(HL^{16})(H_2O)_6\cdot 6H_2O$ (Gd, Er) [62] (Fig. 35). One is 9-coordinate with eight oxygen atoms from four oxalate anions and an aqua ligand. The second one is 8-coordinate with six oxygen atoms from three oxalate anions, a phosphonate oxygen from one $\{HL^{16}\}^-$ anion and an aqua ligand. The third one is 8-coordinate with two oxygen atoms from an oxalate anion, two phosphonate oxygen atoms from two $\{HL^{16}\}^-$ anions and four aqua ligands. The $\{HL^{16}\}^-$ anion is tridentate and bridges with three Ln(III) ions. All phosphonate oxygen atoms are unidentate. All oxalate anions adopt the same coordination mode as that in $Ln_4(C_2O_4)_5(HL^{16})_2(H_2O)_4\cdot 2H_2O$ (Ln = La, Nd).

The interconnection of the first two types of Ln(III) ions by three bridging and chelating oxalate anions lead to a porous 3D network of $Ln_2(C_2O_4)_3$ (Fig. 35b). The large tunnel is formed by 40-member rings composed of 10 Ln(III) ions and 10 oxalate anions. Each pair of the third Ln(III) ions is bridged by two $\{HL^{16}\}^-$ anions to form a dimeric unit, and such units are further interconnected by bridging and chelating oxalate anions into a 1D chain $\{Ln(C_2O_4)(HL^{16})\}$ along *a*-axis (Fig. 35c). These 1D chains of lanthanide(III) oxalate phosphonate as well as the lattice water molecules are located at the large tunnels of $Er_2(C_2O_4)_3$ (Fig. 35d).

The emission spectrum of the Gd(III) exhibits a broad blue fluorescent emission band at $\lambda_{max} = 467$ nm (ex = 375 nm), which corresponds to a ligand-centered (LC) fluorescence. The emission spectrum of the Er(III) compound shows two comparable strong emission bands at 1545 and 1561 nm under 980 nm excitation, both were attributed to the $^4I_{13/2} \rightarrow {}^4I_{15/2}$ transition for the Er^{3+} ion [62].

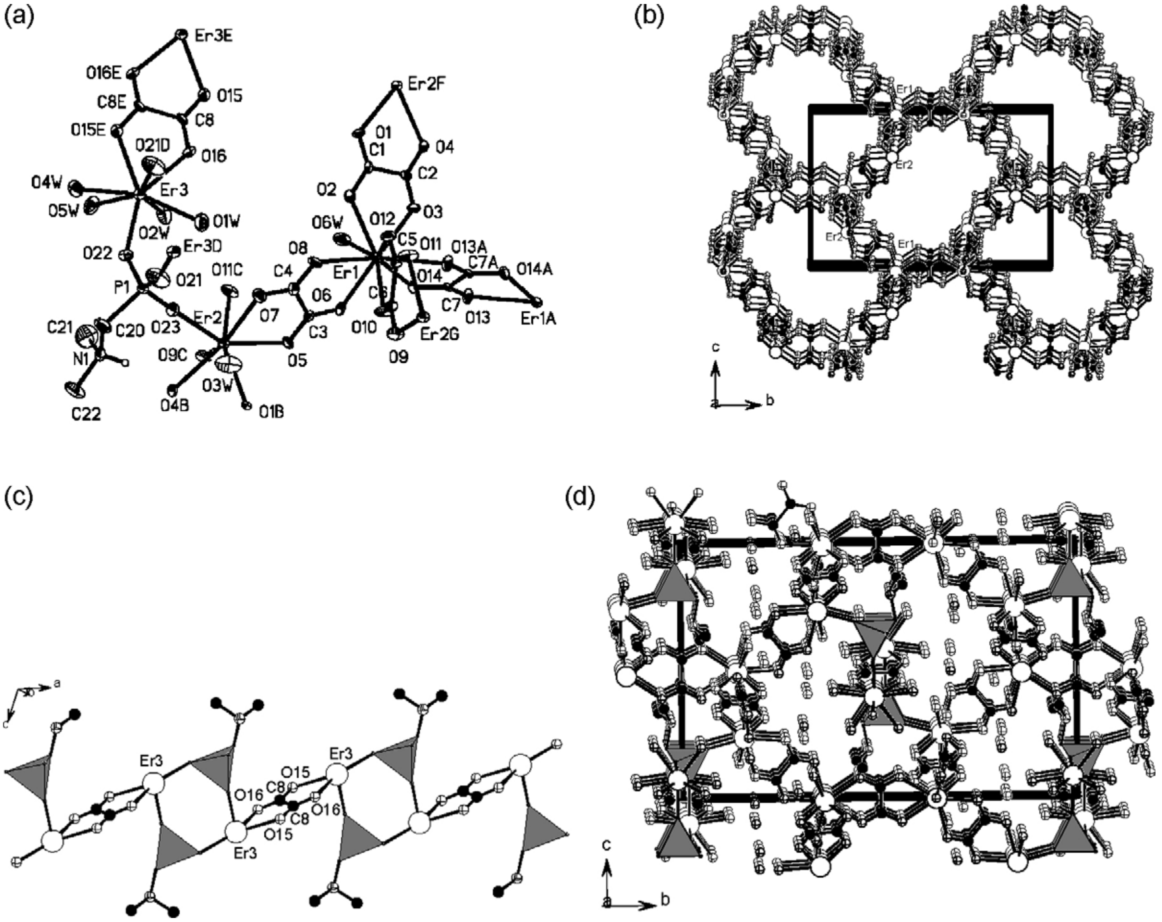

Fig. 35. The selected unit in $Er_3(C_2O_4)_4(HL^{16})(H_2O)_6{\cdot}6H_2O$ (a), a 3D porous network of $Er_2(C_2O_4)_3$ (b) and a 1D chain of $Er(C_2O_4)(HL^{16})$ along *a*-axis (c) and view of the crystal structure of $Er_3(C_2O_4)_4(HL^{16})(H_2O)_6{\cdot}6H_2O$ down the *a*-axis (d) (adapted from Ref. [62]).

Such a synthetic approach can also be extended to the lanthanide tetraphosphonate system whose crystallinity and solubility problem is much more severe. Using $(H_2O_3PCH_2)_2NCH_2CH_2CH_2CH_2N(CH_2PO_3H_2)_2(H_8L^7)$ as the phosphonic acid and oxalate as the second ligand, we were able to prepare three novel lanthanide tetraphosphonates with two types of structures, namely, $La_2(ox)_2(H_6L^7){\cdot}2H_2O$ and $Ln_2(ox)_2(H_6L^7)(H_2O)_2{\cdot}4H_2O$ (Ln = Nd, Eu) [63]. Their structures can also be viewed as lanthanide phosphonate-based networks being decorated by oxalate anions.

The La(III) ion in $La_2(ox)_2(H_6L^7){\cdot}2H_2O$ is 8-coordinate with four oxygen atoms of two chelating oxalate anions, and four phosphonate oxygen atoms of four $\{H_6L^7\}^{2-}$ anions (Fig. 36a). The La–O distances are in the range of 2.419(3) to 2.652(4) Å. Its coordination geometry can be described as a distorted bi-capped trigonal prism. Each oxalate anion is tetradentate and forms two La–O–C–C–O five-member chelating rings. The $\{H_6L^7\}^{2-}$ anion bridges with eight La(III) ions. All four phosphonate groups of the $\{H_6L^7\}^{2-}$ anion are singly protonated, so are the amine groups. The interconnection of La(III) ions by chelating and bridging oxalate anions results in a 1D zigzag chain of $\{La(C_2O_4)\}^+$ along the *a*-axis. The cross-linkage of La(III) ions by bridging $\{H_6L^7\}^{2-}$ anions led to a 3D network with tunnels along *a*-axis (Fig. 36b). A tunnel is formed by 34 member atomic rings composed of four La(III) ions, six phosphonate groups and two N–C–C–C–C–N organic groups (Fig. 36b). The structure of $La_2(ox)_2(H_6L^7){\cdot}2H_2O$ can be described as the oxalate anions occupying and bisecting the tunnels of the lanthanum(III) tetraphosphonate, with the lattice water molecules located at the thus formed small tunnels along the *a*-axis (Fig. 36b).

The structures of $Ln_2(ox)_2(H_6L^7)(H_2O)_2{\cdot}4H_2O$ (Ln = Nd, Eu) feature a different type of 3D network. The Ln(III) is 8-coordinate with four oxygen atoms from two oxalate anions, three phosphonate oxygen atoms from three $\{H_6L^7\}^{2-}$ anions and an aqua ligand (Fig. 37a). The coordination geometry around the Ln(III) ion can be also described as a distorted bi-capped trigonal prism. The $\{H_6L^7\}^{2-}$ anion is hexadentate and bridges with six Ln(III) ions, two of its four phosphonate groups are bidentate whereas the remaining two are unidentate. The oxalate anions form a 1D zigzag $\{Ln(C_2O_4)\}^+$ chain along *b*-axis. The interconnection of Ln(III) ions via bridging $\{H_6L^7\}^{2-}$ anions resulted in a 2D lanthanide phosphonate layer (Fig. 37b). The above two building blocks are interconnected by sharing Ln(III) ions into a pillared-layered architecture with the oxalate groups acting as the pillars, forming narrow-long shaped tunnels along the *b*-axis (Fig. 37c). Alternatively, the structure of $Ln_2(ox)_2(H_6L^7)(H_2O)_2{\cdot}4H_2O$ (Ln = Nd, Eu) can also be viewed as the lanthanide-oxalate-phosphonate hybrid

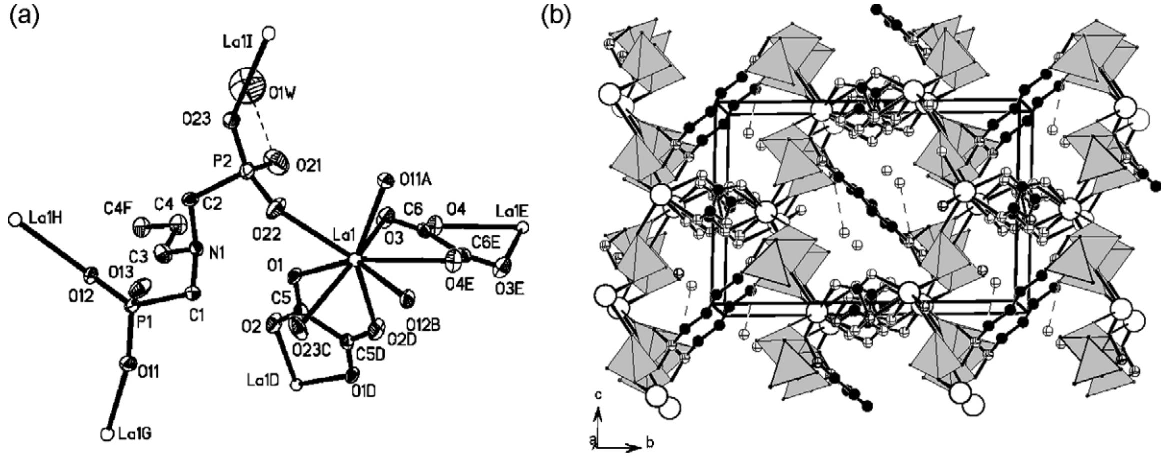

Fig. 36. The selected unit (a) and view of the structure of $[La_2(ox)_2(H_6L^7)]\cdot 2H_2O$ down the *a*-axis (b) (adapted from Ref. [63]).

layers being interconnected by the organic diamine groups (the pillars).

Under excitation of 360 nm, $La_2(ox)_2(H_6L^7)\cdot 2H_2O$ displays a broad blue fluorescent emission band at $\lambda_{max} = 435$ nm, which corresponds to a ligand-centered (LC) fluorescence. $Nd_2(ox)_2(H_6L^7)(H_2O)_2\cdot 4H_2O$ shows the characteristic emission bands for the Nd(III) ion in the near IR region: two moderate emission bands at 875 and 894 nm ($^4F_{3/2} \rightarrow {}^4I_{9/2}$), a very strong emission band at 1056 nm ($^4F_{3/2} \rightarrow {}^4I_{11/2}$) and a very weak band at 1328 nm ($^4F_{3/2} \rightarrow {}^4I_{13/2}$) in the near IR region. $Eu_2(ox)_2(H_6L^7)(H_2O)_2\cdot 4H_2O$ exhibits four sets of characteristic emission bands for the Eu(III) ion in the visible region under excitation at 267 nm: 578.5 nm (very weak, $^5D_0 \rightarrow {}^7F_0$), 587.5, 590.0, 592.5 nm (weak, $^5D_0 \rightarrow {}^7F_1$), 610.5, 617.0, 620.5 nm (very strong, $^5D_0 \rightarrow {}^7F_2$) and 688, 690.5, 694, 698, 701 nm (weak, $^5D_0 \rightarrow {}^7F_4$). The splitting of $^5D_0 \rightarrow {}^7F_1$, $^5D_0 \rightarrow {}^7F_2$, and

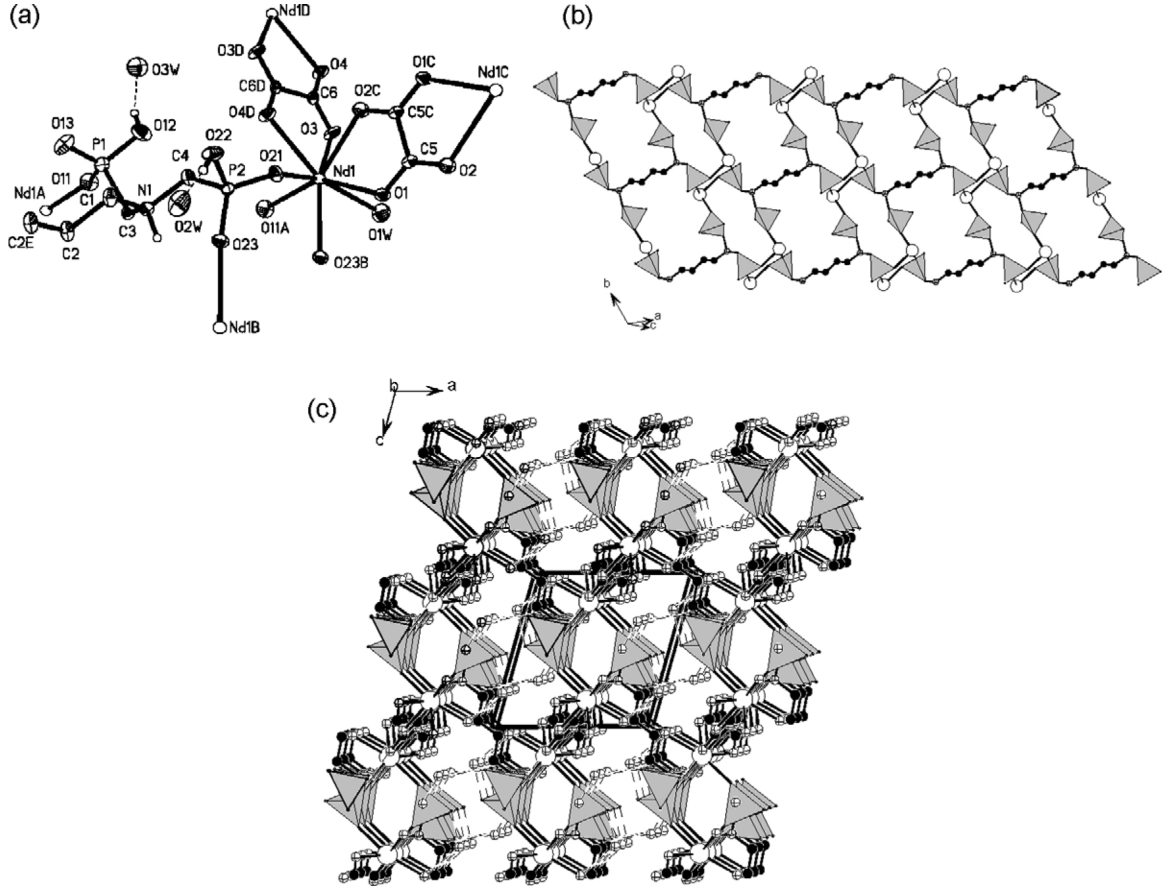

Fig. 37. The selected unit in $Nd_2(ox)_2(H_6L^7)(H_2O)_2\cdot 4H_2O$ (a), a 2D lanthanide(III) tetraphosphonate layer (b) and view of the structure of $Nd_2(ox)_2(H_6L^7)(H_2O)_2\cdot 4H_2O$ down the *b*-axis (c) (adapted from Ref. [63]).

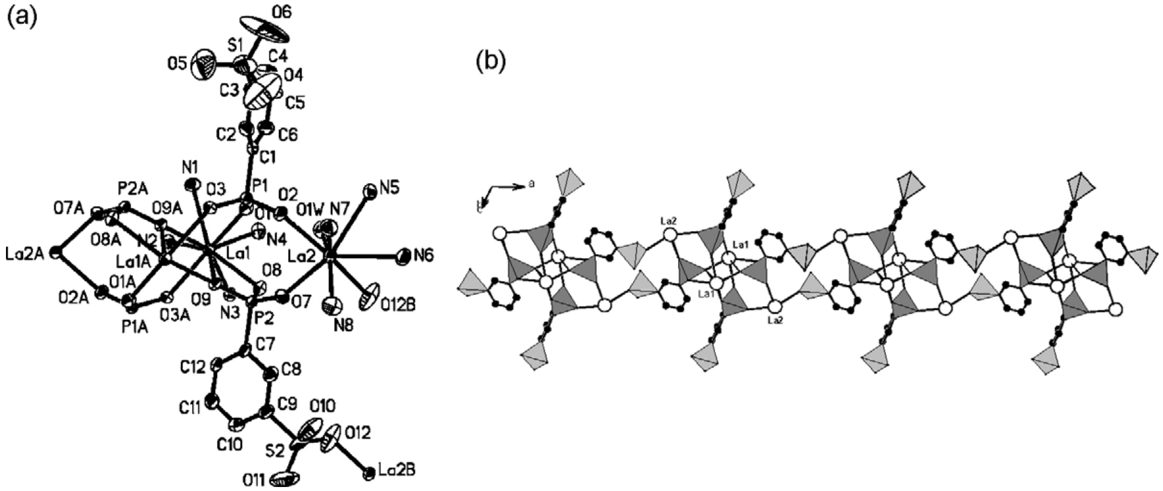

Fig. 38. The selected unit (a) and a 1D cluster chain along the *a*-axis in $[La_2(L^{17})_2(phen)_4(H_2O)]\cdot 4.5H_2O$ (b). The CPO_3 and CSO_3 tetrahedra are shaded in medium and light gray, respectively. La and C atoms are drawn as open and black circles, respectively. The phen ligands and aqua ligands have been omitted for clarity (adapted from Ref. [64]).

$^5D_0 \rightarrow {}^7F_4$ transition bands can be attributed to the "crystal field effect" of the Eu(III) ion in C_1 symmetry, which led to the complete lifting of the degeneracy of the $^7F_1$ and the partial lifting of the degeneracy of the ^7F_j ($j = 2$ and 4) states. The Eu ($^5D_0$) lifetime ($\lambda_{ex,em} = 267, 617$ nm) of $Eu_2(ox)_2(H_6L^7)(H_2O)_2\cdot 4H_2O$ is about 0.38 ms [63].

These studies indicate that we can greatly improve the solubility and crystallinity of lanthanide phosphonates by introducing acidic carboxylate or sulfonate ligand as the second metal linker. Such a synthetic technique also allows us to design new types of lanthanide complexes with novel crystal structures and luminescent properties.

Basic ligands such as 1,10-phen can also act as the second metal linker, the coordination of such chelating ligand to the lanthanide(III) ion reduces the coordination sites available for the phosphonate ligand, thus cluster compounds could be isolated. By using *m*-HO_3S–C_6H_4–PO_3H_2(H_3L^{17}) as the primary ligand and 1,10-phenanthroline (phen) or *N*,*N*′-piperazinebis(methylenephosphonic acid) (H_4L^2) as the auxiliary ligand, six novel lanthanide(III) sulfonate-phosphonates based on two types of tetranuclear clusters, namely, $[La_2(L^{17})_2(phen)_4(H_2O)]\cdot 4.5H_2O$, $[Ln_2(L^{17})_2(phen)_2(H_2O)_5]\cdot 3H_2O$ (Ln = Nd, Eu, Er) and $[Ln_2(HL^{17})(H_2L^2)_2(H_2O)_4]\cdot 8H_2O$ (Ln = La, Nd) were isolated [64]. Their structures feature isolated, 1D and 3D tetranuclear lanthanide clusters.

$[La_2(L^{17})_2(phen)_4(H_2O)]\cdot 4.5H_2O$ features a 1D chain of clusters (Fig. 38). There are two unique La(III) ions in the asymmetric unit, La(1) is 9-coordinate whereas La(2) is 8-coordinate (Fig. 38a). Among two crystallographically distinct $\{L^{17}\}^{3-}$

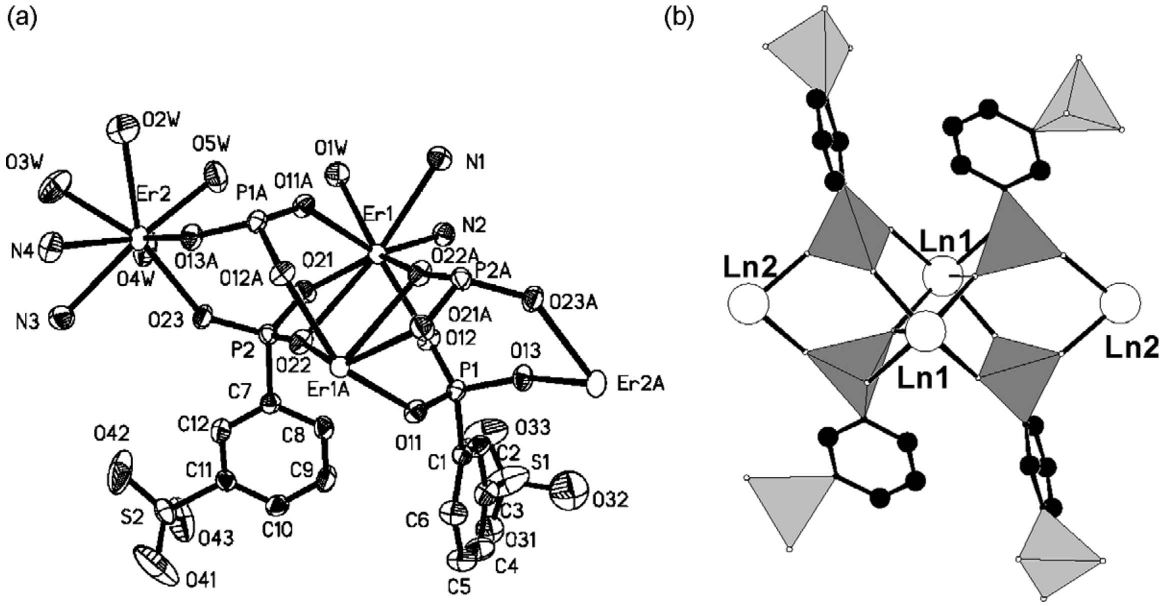

Fig. 39. The selected unit in $[Er_2(L^{17})_2(phen)_2(H_2O)_5]\cdot 3H_2O$ (a) and a tetranuclear cluster in $[Ln_2(L^{17})_2(phen)_2(H_2O)_5]\cdot 3H_2O$ (Ln = Nd, Eu, Er) (b). The CPO_3 and CSO_3 tetrahedra are shaded in medium and light gray, respectively. The phen ligands and aqua ligands have been omitted for clarity (adapted from Ref. [64]).

anions, one is tridentate with each phosphonate oxygen bridging to a La(III) ion and the other $\{L^{17}\}^{3-}$ anion is pentadentate by using its three phosphonate oxygen atoms and one sulfonate oxygen. The phosphonate group is tetradentate and bridges with three La(III) ions, one phosphonate oxygen atom functions as a μ^2-metal linker. The sulfonate group is unidentate. Two La(1) and two La(2) ions are interconnected by four phosphonate groups of four $\{L^{17}\}^{3-}$ anions into a tetranuclear cluster unit (Fig. 38b). The distances of La(1)···La(2) edges are 5.809(1) and 5.887(1) Å, respectively and the La(1)···La(1) distance is 4.063(1) Å. Each phosphonate ligand caps on a La_3 triangle. This tetranuclear cluster is connected to two neighboring ones through the coordination of the sulfonate oxygen atoms, forming a 1D chain along the *a*-axis (Fig. 38b).

When the La(III) ions were replaced by other Ln(III) ions, $[Ln_2(L^{17})_2(phen)_2(H_2O)_5]\cdot 3H_2O$ (Ln = Nd, Eu, Er) were isolated. These compounds feature discrete tetranunuclear lanthanide(III) cluster (Fig. 39). There are two unique Ln(III) ions in the asymmetric unit, both are 8-coordinate (Fig. 39a). The phosphonate groups of the $\{L^{17}\}^{3-}$ ligands adopt the same coordination fashion as those in the lanthanum compound. However the sulfonate group remains uncoordinated. Four lanthanide(III) ions are bridged by four sulfonate-phosphonate ligands into a similar tetranuclear cluster (Fig. 39b). These clusters are isolated due to the uncoordinated nature of the sulfonate groups.

$[Ln_2(HL^{17})(H_2L^2)_2(H_2O)_4]\cdot 8H_2O$ (Ln = La, Nd) were isolated when *N*,*N*′-piperazinebis (methylenephosphonic acid) was applied as the second metal linker instead of phen and the reaction media is more acidic. Their structures features a 3D architecture based on a different type of lanthanide tetranuclear clusters (Fig. 40). Among two unique Ln(III) ions, one is 8-coordinate with six phosphonate oxygen atoms from four $\{H_2L^2\}^{2-}$ anions and two phosphonate oxygen atoms from two $\{HL^{17}\}^{2-}$ anions, whereas the other one is 9-coordinate with three phosphonate oxygen atoms from two $\{HL^{17}\}^{2-}$ anion, two phosphonate oxygen atoms from two $\{H_2L^2\}^{2-}$ anions as well as four aqua ligands (Fig. 40a). The phosphonate group of the $\{HL^{17}\}^{2-}$ anion is pentadentate, two phosphonate oxygen atoms act as μ^2-bridging ligand whereas the third oxygen atom is monodentate. The sulfonate group of the $\{HL^{17}\}^{2-}$ anion is severely disordered and remains uncoordinated. Each $\{HL^{17}\}^{2-}$ anion connects with four Ln(III) ions. The two $\{H_2L^2\}^{2-}$ anions adopt two different coordination modes: one is tetradentate and bridges with four Ln(III) ions from two cluster units and the

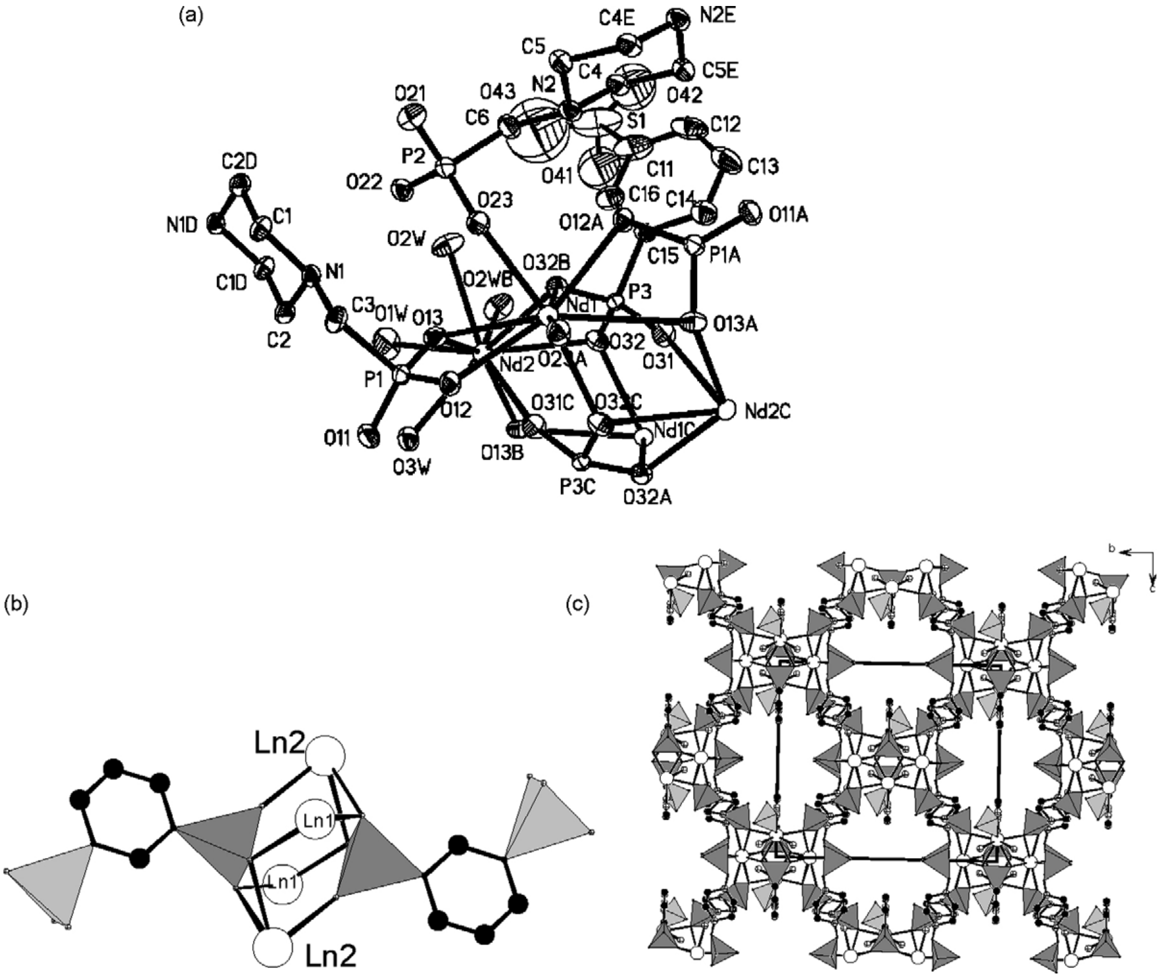

Fig. 40. The selected unit in $[Ln_2(HL^{17})(H_2L^2)_2(H_2O)_4]\cdot 8H_2O$ (a), a tetranuclear $\{Ln_4(HL^{17})_2\}^{4+}$ cluster (b) and the 3D open framework (c) in $[Ln_2(HL^{17})(H_2L^2)_2(H_2O)_4]\cdot 8H_2O$ (Ln = La, Nd). The CPO_3 and CSO_3 tetrahedra are shaded in medium and light gray, respectively. The lattice water molecules have been omitted for clarity (adapted from Ref. [64]).

other one is bidentate and connects with two Ln(III) ions from two cluster units. The interconnection of four Ln(III) ions by two bridging $\{HL^{17}\}^{2-}$ anions resulted in a $\{Ln_4(HL^{17})_2\}^{4+}$ tetranuclear cluster (Fig. 40b). The four Ln(III) ions form a slightly distorted square with the two phosphonate groups of $\{HL^{17}\}^{2-}$ ligands capping above and below the square. Each Ln(1)···Ln(2) edge is further bridged by a phosphonate group of a $\{H_2L^2\}^{2-}$ anion. The Ln(1)···Ln(2) edges are significantly shorter than those in first type of tetranuclear cluster. Such clusters are further cross-linked by the bridging $\{H_2L^2\}^{2-}$ anions into a 3D open framework with larger tunnels along the *a*-axis (Fig. 40c). Each cluster is bridged to six neighbors. The lattice water molecules are located in the above tunnels. The total solvent accessible spaces are about 23.8% and 23.3% of the cell volume for the La and Nd compounds, respectively. The open framework of the La compound remains intact after heating at 150 °C for 4 h based on XRD powder studies [64].

Under excitation at 335 nm, $[Nd_2(L^{17})_2(phen)_2(H_2O)_5]\cdot 3H_2O$ displays three sets of characteristic emission bands for the neodymium(III) ion: 890 and 879 nm ($^4F_{3/2} \rightarrow {}^4I_{9/2}$), 1061 and 1072 nm ($^4F_{3/2} \rightarrow {}^4I_{11/2}$) and a weak band at 1335 nm ($^4F_{3/2} \rightarrow {}^4I_{13/2}$) in the near IR region. $[Eu_2(L^{17})_2(phen)_2(H_2O)_5]\cdot 3H_2O$ exhibits three strong characteristic emission bands for the europium(III) ion in the visible region under excitation at 337 nm: 535 nm ($^5D_0 \rightarrow {}^7F_0$), 591 nm ($^5D_0 \rightarrow {}^7F_1$), 615 nm ($^5D_0 \rightarrow {}^7F_2$) and 685 nm ($^5D_0 \rightarrow {}^7F_4$). The Eu ($^5D_0$) lifetime for $\lambda_{ex,em} = 337$, 614 nm was measured to be 0.29 ms [64].

In summary, the introduction of a second metal linker is an effective route to lanthanide phosphonates with interesting structures and novel luminescent properties. The basic second ligand such as phen can limit the coordination sites of the lanthanide ion available for the phosphonate ligand and hence facilitate the formation of lanthanide compounds with polynuclear cluster units. For acidic second ligand such as oxalate, the lanthanide compounds obtained usually display complicated 3D network structure, the second ligand can be incorporated into the open framework of lanthanide phosphonates (primary ligand dominated) or the phosphonate ligand being incorporated into the open framework formed by the lanthanide ions and the second ligands (second ligand-dominated).

7. Concluding remarks and outlook

The above discussion demonstrates that lanthanide phosphonates can exhibit a variety of structural features ranging from clusters, 1D chains, 2D layers to 3D networks similar to transition metal phosphonates. The solubility and crystallinity of lanthanide phosphonates can be enhanced by attaching various functional groups to phosphonic acids or introducing a second metal linker. By using these synthetic techniques we could design lanthanide phosphonates with excellent luminescent properties. The use of an acidic second metal linker, such as oxalic acid, usually results in open framework structures whereas the use of a basic second ligand such as 1,10-phen can lead to the formation of lanthanide(III) phosphonates with polynuclear cluster units. Phosphonate ligands in lanthanide complexes are flexible ligands which can adopt a number of coordination modes depending on many factors such as the reaction temperature, pH value of the reaction media, the type of counteranion and the size of the lanthanide cation, as displayed by the lanthanide phosphonates in references [49,50].

The chemistry of lanthanide phosphonates will remain an active research area. The phosphonate ligand is able to bind with both transition and lanthanide metals, therefore we believe that it is feasible to prepare lanthanide-transition metal phosphonates which may possess novel magnetic and luminescent properties as well as novel structural architectures. The design of chiral lanthanide phosphonates is also of special interest due to their possible applications in heterogeneous catalysis and chiral separations. The search for lanthanide phosphonates with excellent luminescent properties in the near IR region is also important due to their potential applications in telecommunications. Furthermore, lanthanide phosphonates could be developed as nanomaterials, as demonstrated recently by Ma and coworkers, that nanoparticles and nanorods of lanthanide phenylphosphonate were successfully prepared by low-temperature hydrothermal methods [65].

Acknowledgements

This work was supported by the National Natural Science Foundation of China (Nos. 20371047, 20573113 and 20521101), NSF of Fujian Province (No. E0420003) and Key Project from Chinese Academy of Sciences. I am grateful to Prof. Ji-Wen Cai of Sun Yat-Sen University for her great help. I am also indebted to my graduate students, Jun-Ling Song, Chong Lei, Shaoming Ying, Zi-Yi Du and Si-Fu Tang for their productive work.

References

[1] A. Clearfield, in: K.D. Karlin (Ed.), Progress in Inorganic Chemistry, vol. 47, John Wiley & Sons, New York, 1998, p. 371 (and references therein).
[2] A.K. Cheetham, G. Férey, T. Loiseau, Angew. Chem. Int. Ed. 38 (1999) 3269.
[3] J. Zhu, X. Bu, P. Feng, G.D. Stucky, J. Am. Chem. Soc. 122 (2000) 11563.
[4] F. Fredoueil, M. Evain, D. Massiot, M. Bujoli-Doeuff, P. Janvier, A. Clearfield, B. Bujoli, J. Chem. Soc., Dalton Trans. (2002) 1508.
[5] P. Rabu, P. Janvier, B. Bujoli, J. Mater. Chem. 9 (1999) 1323.
[6] N. Stock, S.A. Frey, G.D. Stucky, A.K. Cheetham, J. Chem. Soc., Dalton Trans. (2000) 4292.
[7] S. Ayyappan, G.D. Delgado, A.K. Cheetham, G. Férey, C.N.R. Rao, J. Chem. Soc., Dalton Trans. (1999) 2905.
[8] S.J. Hartman, E. Todorov, C. Cruz, S.C. Sevov, Chem. Commun. (2000) 1213.
[9] J.-G. Mao, Z. Wang, A. Clearfield, Inorg. Chem. 41 (2002) 2334.
[10] J.-G. Mao, Z. Wang, A. Clearfield, Inorg. Chem. 41 (2002) 3713.
[11] J.-G. Mao, Z.K. Wang, A. Clearfield, Inorg. Chem. 41 (2002) 6106.
[12] P. Yin, L.M. Zheng, S. Gao, X.-Q. Xin, Chem. Commun. (2001) 2346.
[13] L.-M. Zheng, S. Gao, H.-H. Song, S. Decurtins, A.J. Jacobson, X.-Q. Xin, Chem. Mater. 14 (2002) 3143.
[14] L.-M. Zheng, P. Yin, X.-Q. Xin, Inorg. Chem. 41 (2002) 4084.
[15] E. Burkholder, V. Golub, C.J. O'Connor, J. Zubieta, Chem. Commun. (2003) 2128.
[16] R.C. Finn, E. Burkholder, J. Zubieta, Chem. Commun. (2001) 1852.
[17] R.C. Finn, J. Zubieta, Inorg. Chem. 40 (2001) 2466.
[18] R.C. Finn, E. Burkholder, J. Zubieta, Inorg. Chem. 40 (2001) 3745.

[19] C. Lei, J.-G. Mao, Y.-Q. Sun, H.-Y. Zeng, A. Clearfield, Inorg. Chem. 42 (2003) 6157.

[20] J.-L. Song, J.-G. Mao, Y.-Q. Sun, A. Clearfield, Eur. J. Inorg. Chem. (2003) 4218.

[21] J.L. Song, H.H. Zhao, J.-G. Mao, K.R. Dunbar, Chem. Mater. 16 (2004) 1884.

[22] C.N.R. Rao, S. Natarajan, R. Vaidhyanathan, Angew. Chem. Int. Ed. 43 (2004) 1466.

[23] K. Maeda, Micro. Meso. Mater. 73 (2004) 47.

[24] E. Matczak-Jon, V. Videnova-Adrabińska, Coord. Chem. Rev. 249 (2005) 2458.

[25] F.S. Richardson, Chem. Rev. 82 (1982) 541.

[26] W.D. Horrocks Jr., D.R. Sudnik, J. Am. Chem. Soc. 101 (1979) 334.

[27] G. Cao, V.M. Lynch, J.S. Swinnea, T.E. Mallouk, Inorg. Chem. 29 (1990) 2112.

[28] R.-C. Wang, Y. Zhang, H. Hu, R.R. Frausto, A. Clearfield, Chem. Mater. 4 (1992) 864.

[29] S.R. Miller, E. Lear, J. Gonzalez, A.M.Z. Slawin, P.A. Wright, N. Guillou, G. Férey, Dalton Trans. (2005) 3319.

[30] F. Serpaggi, G. Férey, J. Mater. Chem. 8 (1998) 2749.

[31] E. Antic-Fidancev, F. Serpaggi, G. Férey, J. Alloys Chem. 319 (2001) 140.

[32] F. Serpaggi, G. Férey, F. Antic-Fidancev, J. Solid State Chem. 148 (1999) 347.

[33] O.R. Evans, H.L. Ngo, W. Lin, J. Am. Chem. Soc. 123 (2001) 10395.

[34] T. Głowiak, E. Huskowska, J. Legendziewicz, Polyhedron 10 (1991) 175.

[35] J.A. Groves, P.A. Wright, P. Lightfoot, Inorg. Chem. 44 (2005) 1736.

[36] J.A. Groves, N.F. Stephens, P.A. Wright, P. Lightfoot, Solid State Sci. 8 (2006) 397.

[37] S. Comby, R. Scopelliti, D. Imbert, L. Charbonnière, R. Ziessel, J.C.G. Bünzli, Inorg. Chem. 45 (2006) 3158.

[38] D.-K. Cao, Y.-Z. Li, Y. Song, L.-M. Zheng, Inorg. Chem. 44 (2005) 3599.

[39] X.M. Gan, I. Bingamin, B.M. Rapko, J. Fox, E.N. Duesler, R.T. Paine, Inorg. Chem. 43 (2004) 2443.

[40] X.-M. Gan, B.M. Rapko, J. Fox, I. Binyamin, S. Pailloux, E.N. Duesler, R.T. Paine, Inorg. Chem. 45 (2006) 3741.

[41] S.-M. Ying, X.-R. Zeng, X.-N. Fang, X.-F. Li, D.-S. Liu, Inorg. Chim. Acta 359 (2006) 1589.

[42] K.L. Nash, R.D. Rogers, J. Ferraro, J. Zhang, Inorg. Chem. Acta 269 (1998) 211.

[43] J.-P. Silvestre, N.Q. Dao, M.-R. Lee, Phosphorus, Sulfur, Silicon, Relat. Elem. 176 (2001) 173.

[44] X.-M. Gan, I. Binyamin, S. Pailloux, E.N. Duesler, R.T. Paine, Dalton Trans. (2006) 3912.

[45] J. Legendziewicz, P. Gawryszewska, E. Gałdecka, Z. Galdecki, J. Alloy Compd. 275–277 (1998) 356.

[46] E. Gałdecka, Z. Gałdecki, P. Gawryszewska, J. Legendziewicz, New J. Chem. 24 (2000) 387.

[47] F. Serpaggi, G. Férey, Inorg. Chem. 38 (1999) 4741.

[48] C. Serre, N. Stock, T. Bein, G. Ferey, Inorg. Chem. 43 (2004) 3159.

[49] S.-F. Tang, J.-L. Song, J.-G. Mao, Eur. J. Inorg. Chem. (2006) 2011.

[50] S. Bauer, T. Bein, N. Stock, J. Solid State Chem. 179 (2006) 145.

[51] S. Bauer, T. Bein, N. Stock, Inorg. Chem. 44 (2005) 5882.

[52] Q. Yue, J. Yang, G.-H. Li, G.-D. Li, J.-S. Chen, Inorg. Chem. 45 (2006) 4431.

[53] S.-F. Tang, J.-L. Song, X.-L. Li, J.-G. Mao, Cryst. Growth Des. 6 (2006) 2322.

[54] A. Clearfield, C.V.K. Sharma, B. Zhang, Chem. Mater. 13 (2001) 3099.

[55] H.L. Ngo, W. Lin, J. Am. Chem. Soc. 124 (2002) 14298.

[56] J. Plutnar, J. Rohovec, J. Kotek, Z. Žák, I. Lukeš, Inorg. Chem. Acta 335 (2002) 27.

[57] J. Rudovský, P. Cígler, J. Kotek, P. Hermann, P. Vojtíšek, I. Lukeš, J.A. Peters, L. Vander Elst, R.N. Muller, Chem. Eur. J. 11 (2005) 2373.

[58] P. Vojtíšek, P. Cígler, J. Kotek, J. Rudovský, P. Hermann, I. Lukeš, Inorg. Chem. 44 (2005) 5591.

[59] S.W.A. Bligh, N. Choi, C.F.G.C. Geraldes, S. Knoke, M. McPartlin, M.J. Sanganee, T.M. Woodroffe, J. Chem. Soc., Dalton Trans. (1997) 4119.

[60] F. Avecilla, J.A. Peters, C.F.G.C. Geraldes, Eur. J. Inorg. Chem. (2003) 4179.

[61] J.L. Song, C. Lei, J.G. Mao, Inorg. Chem. 43 (2004) 5630.

[62] J.L. Song, J.G. Mao, Chem. Eur. J. 11 (2005) 1417.

[63] S.-M. Ying, J.-G. Mao, Cryst. Growth Des. 6 (2006) 964.

[64] Z.-Y. Du, H.-B. Xu, J.-G. Mao, Inorg. Chem. 45 (2006) 9780.

[65] S.-Y. Song, J.-F. Ma, J. Yang, M.-H. Cao, H.-J. Zhang, H.-S. Wang, K.-Y. Yang, Inorg. Chem. 45 (2006) 1201.